

A REPORT ON  
**STUDIES OF TASAR SILK FIBROIN/ BIOACTIVE CLAY  
NANOCOMPOSITE FILMS**  
A MAJOR PROJECT THESIS  
SUBMITTED IN PARTIAL FULFILLMENT OF THE REQUIREMENTS  
FOR THE AWARD OF THE DEGREE OF  
**MASTER OF TECHNOLOGY**  
IN  
**POLYMER TECHNOLOGY**

**Submitted By: NARENDRA KUMAR**

2K17/PTE/04

**Under the supervision of**

**Dr. Roli Purwar**



**DEPARTMENT OF APPLIED CHEMISTRY  
DELHI TECHNOLOGICAL UNIVERSITY**

Bawana Road, Delhi-110042

JUNE, 2019

# DELHI TECHNOLOGICAL UNIVERSITY

(Formerly Delhi College of Engineering)

## Department of Applied Chemistry

Shahbad Daultapur, Bawana Road, Delhi – 110042, India



## DECLARATION

I hereby declare that the work presented in this major project report entitled “**STUDIES OF TASAR SILK FIBROIN/ BIOACTIVE CLAY NANOCOMPOSITE FILMS**” is original and has been carried out by me in the partial fulfillment of the requirement for the award of the Master of Technology in Polymer Technology in the Department of Applied Chemistry, Delhi Technological University, Delhi – 110042, under the supervision of **Dr. Roli Purwar**, Associate Professor, Department of Applied Chemistry. This report is contribution of my original research work. Wherever research contributions of others are involved, every effort has been made to clearly indicate the same. To the best of my knowledge, this research work has not been submitted in part or full for the award of any degree or diploma of Delhi Technological University or any other University/Institution.

**NARENDRA KUMAR**

**2K17/PTE/04**

# DELHI TECHNOLOGICAL UNIVERSITY

(Formerly Delhi College of Engineering)

Shahbad Daultapur, Bawana Road, Delhi – 110042, India



## CERTIFICATE

This is to certify that the work presented in this major project report entitled “**STUDIES OF TASAR SILK FIBROIN/ BIOACTIVE CLAY NANOCOMPOSITE FILMS**” has been submitted to the Delhi Technological University, Delhi-110042, in fulfilment for the requirement for the award of the degree of **M.Tech in Polymer Technology** by the candidate **NARENDRA KUMAR, (2K17/PTE/04)** under the supervision of **Dr Roli Purwar, Associate Professor,** Department of Applied Chemistry. It is further certified that the work embodied in this report has neither partially nor fully submitted to any other university or institution for the award of any degree or diploma.

**Place:**

**Date:**

**(Dr. Roli Purwar)**

Supervisor

## **ACKNOWLEDGEMENT**

The success and final outcome of this project required a lot of guidance and assistance from many people and I am extremely fortunate to have got this all along the completion of this project work.

I wish to express my gratitude towards my project supervisor, **Dr.Roli Purwar, Department of Applied Chemistry, Delhi Technological University**, who provided me a golden opportunity to work under her able guidance. Her scholastic guidance and sagacious suggestions helped me to complete the project on time.

I wish to thank **Dr. Archna Rani, Professor and Head of the Department of Applied Chemistry, Delhi Technological University**, for her constant motivation and for providing able guidance.

I am thankful to and fortunate enough to get constant encouragement, support and guidance from all teaching as well as non-teaching staffs of Department of Applied Chemistry and Polymer Technology, which helped me in successfully completing my project work.

Finally, yet importantly, I would like to express my heartfelt thanks to my beloved family and friends who have endured my long working hours and whose motivation kept me going.

**NARENDRA KUMAR**

## **TABLE OF CONTENT**

<b>S.NO.</b>	<b>TITLE</b>	<b>PAGE. NO.</b>
1.	INTRODUCTION AND OBJECTIVE	1-4
2.	LITERATURE REVIEW	5-28
3.	EXPERIMENTAL WORK	29-33
4.	RESULT AND DISCUSSION	34-49
5.	CONCLUSION	50
6.	REFERENCES	51-54

## LIST OF TABLES:

S.NO.	TITLE	PAGE. NO.
<b>Table 1</b>	Molecular Weight and Tensile Strength of Silk Proteins (Fibroin and Sericin) Isolated from Different Mulberry and Nonmulberry Species	10
<b>Table 2</b>	Major groups of clay minerals:	18
<b>Table 3</b>	Important physical properties Of montmorillonite clay:	21
<b>Table 4</b>	particles size of different types of modified MMT clay	35
<b>Table 5</b>	Antibacterial activity of Cu-MMT clay :	42
<b>Table 6</b>	Antibacterial activity of Ag-MMT clay:	44
<b>Table 7</b>	Antibacterial activity of Quat. Ammo.--MMT clay:	44
<b>Table 8</b>	Antibacterial activity of Tasar silk fibroin/Ag—MMT nanocomposite film:	45
<b>Table 9</b>	Antibacterial activity of Tasar silk fibroin/Cu—MMT nanocomposite film:	45
<b>Table 10</b>	Antibacterial activity of Tasar silk fibroin/Quat. Ammo.—MMT nanocomposite film:	45

## LIST OF FIGURES

S.NO.	TITLE	PAGE NO.
Figure 1:	Typical life cycle/ different stages of nonmulberry indian tropical tasar silkworm, <i>ANTHERAEA MYLITTA</i>	7
Figure 2:	The cocoon of of wild Indian tropical nonmulberry silkworm, <i>Antheraea mylitta</i> attached to twig of host plant with the help of peduncle (in the form of a ring to hold the tree branches), which is spun first.	8
Figure 3:	Montmorillonite clay structure	20
Figure 4:	Dissolution of degummed tasar silk fibroin in ionic liquid with continuous stirring	30
Figure 5:	Preparation of tasar silk fibroin/bioactive clay nanocomposite films	30
Figure 6:	TGA of different modified mmt clay and tasar silk/bioactive clay nanocomposite films	34
Figure 7:	SEM and EDX of silver modified clay	37
Figure 8:	SEM and EDX of copper modified clay	38
Figure 9:	SEM and EDX of Quat. Ammo. modified clay	39
Figure 10:	TEM of tasar silk fibroin/ bioactive clay nanocomposite films	40
Figure 11:	FTIR of tasar silk fibroin/bioactive clay nanocomposite films	41
Figure 12:	microbial colonies formation during antibacterial testing	43
Figure 13:	XRD of pristine Na-MMT and Ag-MMT clay	46
Figure 14:	XRD of pristine Cu-MMT and Quat. Ammo-MMT clay	47
Figure 15:	XRD of tasar silk/ bioactive clay nanocomposite films	48

## **ABSTRACT**

The purpose of our research is creating a new nanocomposite material using tasar silk fibroin and modified montmorillonite (MMT) clay. Generally, the silk fibroin is started as a promising base material for biomedical applications. The incorporation of montmorillonite (MMT) into silk fibroin would improve physical properties of the silk fibroin and impart antibacterial properties. We investigated tasar silk fibroin with MMT for the different types of physical properties. Specifically, tasar silk fibroin were dissolved in ionic liquid and by mixing certain amounts of modified MMT clay to obtain a bionanocomposite. Their ultrastructure were successfully visualized by transmission electron microscopy. The morphology and particle size of modified MMT clay was examined using scanning electron microscopy and particle size analyzer. This nanocomposite was comprised of intercalated thin layers of MMT, each with a thickness of about 1.66nm which is confirmed by XRD results. We also performed TGA and FTIR analysis in conjunction with morphological data for characterization. Convincingly we obtained a new bionanocomposite of tasar silk fibroin and MMT, which has never been reported. This unique nanocomposite possess antibacterial properties which can make it be useful as scaffold for biological tests in tissue engineering.



## I. INTRODUCTION

Silk, protein fiber spun by a variety of insects in nature, has been used for thousands years as a luxury clothing materials because of its texture, mechanical strength, and optical luster. Raw silk fiber contains a fibrous protein known as fibroin, which forms a thread core, and glue-like proteins called sericin that surround the fibroin fibers to cement them together. There are four different varieties of silk fibroin namely, mulberry, tasar, muga, and eri obtained from *bombyx mori*, *A.mylita*, *A.assama*, *A.perini* respectively. Tasar, muga and eri silk are known as wild variety of silk or non-mulberry silk. In last two decades the use of silk fibroin has been expanded in the wide variety of biomedical applications in the form of films, hydrogels, fibrous sponges and nonwoven mats. In order to achieve in different physical form, silk fibroin need to be dissolved in adequate solvent and regenerated.

The tasar variety of silk has been found in the Indian subcontinent. Tasar fibroin obtain from silkworm gland has been studied extensively and found potential candidate for biomedical applications due to its biocompatible and biodegradable properties and other mechanical properties. Tasar silk fibroin can be dissolved in ionic liquids. our research group have developed regenerated flexible films, nonwoven fibrous mats using tasar fibroin obtained from cocoons for wound dressing and skin tissue engineering applications.

The presence of hydrophobic regions within the silk fibroin are responsible for the formation of antiparallel  $\beta$ -sheet secondary structure that control the mechanical properties of silk. During regeneration process, the crystallinity can be induced through chemical or physical treatments and the degree of crystallinity specifies silk degradation rates and stability in aqueous and organic solvents.

Clay minerals are platelets of layered silicates with a high surface area and high aspect ratios. Montmorillonite (MMT), also known as clay, is one of the most commonly used layered silicates, with the general formula  $M_x(Al_{4-x}Mg_x)Si_8O_{20}$  and a crystal lattice of octahedral sheets of alumina or magnesium fused between two tetrahedral silica sheets. The crystal layers are about 1nm thick and up to several microns long and organize into stacks with a separating gap filled with alkaline metals that can be easily exchanged with small molecules. Due to its abundance, environmental friendliness and well-studied chemistry, montmorillonite (MMT) has gained prominence due to

its reinforcing property. The studies revealed that larger surface area and large aspect ratio are the salient attributes responsible for the reinforcement.

Montmorillonite show no antibacterial effect, however, they could kill adsorbed bacteria when an antibacterial material was intercalated in or adsorbed on them. Studies on the modification of clay minerals as inorganic carriers or antibacterial agents have been extensively reported. For instance, clay minerals could be loaded with inorganic species exhibiting antibacterial properties, such as silver ions, copper and zinc ions or with an organic antibacterial agent such as cetylpyridinium bromide (CPB) and chlorhexidine acetate (CA).[1]–[3]

Bionanocomposites are organic-inorganic hybrid nanostructured materials with synergistic properties that result from the combination of bioderived (natural polymers) and inorganic components. Multifunctionalities of Bionanocomposites make them quite interesting for applications in different fields such as packaging, catalysis, optics, electronics, biomedicine, tissue engineering and drug delivery. Among the wide range of biomaterials, natural protein silk fibroin (SF) from *Bombyx mori* cocoon is a suitable candidate for the development of untraditional bionanocomposites for biomedical and technological applications. Among these forms, in high-tech devices, silk fibroin film has found growing integration applications. The combination of natural polymers (proteins) and inorganic solids (e.g., clays) has become an emerging group of hybrid materials, namely, bionanocomposites.[4]

A silk fibroin and montmorillonite(SF-MMT) nanocomposites with good clay dispersion was obtained by changing the solution pH value below the silk fibroin isoelectric point (pI), the SF in the cation state was able to interact strongly with unmodified anionic montmorillonite (MMT) surface[5]. It is described the formation of silk protein / clay composite biomaterials for formation of bone tissue. [6]

By combining hydroxalcite-like compounds and silk fibroin (SF-HTlc) through an environmentally friendly aqueous process, hybrid functional materials are formed.[4]

Thus from the existing literature search, it has been found that there have been no studies on the use of regenerated tasar fibroin/bioactive clay nanocomposite films obtained from cocoons.

## **Motivation of research**

Nonmulberry silk fibroin proteins are found to be potential biomaterials; however the studies on tasar silk fibroin/bioactive clay nanocomposites film is not reported in the literature. India is the largest producer of nonmulberry silk fibroin protein and most of present studies are confined to nonmulberry silk fibroin proteins extracted from silkworm gland. It is very difficult to develop the biomedical products for commercial use from the protein obtained from silkworm gland. Therefore, there is a need to study the properties of regenerated nonmulberry silk fibroin extracted from cocoon with the bioactive clay nanocomposites films to explore its applications.

## **Objective:**

Preparation and characterization of regenerated nonmulberry tasar silk fibroin/bioactive clay nanocomposites films.

## **Specific Objectives:**

In order to achieve the above objective, the specific objectives are:

- Preparation of the bioactive clay modified with copper , silver and quaternary ammonium salts
- Characterization of the bioactive clay using TGA, SEM-EDX, XRD and particle size analysis
- Evaluation of antibacterial properties of the modified bioactive clay.
- Preparation of tasar silk/ bioactive clay nanocomposite film using solution casting method
- Characterization of nanocomposites film using FTIR, TGA, TEM, and XRD.
- Evaluation of antibacterial properties of the nanocomposites film for biomedical applications.

## II. LITERATURE REVIEW

The lepidopterans belonging to the Bombyciidae and Saturniidae families has been commercially exploited to produce silk in different pockets of our country. Silkworms are classified as mulberry (e.g. *Bombyx mori*) and non-mulberry types (e.g. *Antheraea mylitta*, *Antheraea assamensis*, *Philosamia ricini*) depending on the habit of feeding. The silkworms of mulberry, *B. Mori* (Bombyciidae) feed on mulberry leaves and contribute approximately 90% of global silk production. There are plenty of reports on the protocols and associated challenges of cultivating the domesticated mulberry silkworm and studies on its protein chemistry, genome and exploitation in various fields including tissue engineering, drug delivery and nanobiotechnology. Some of the representative works involving *B. mori* silk biomaterials has been presented. A simple prototype device for the directional freezing of *B. mori* was manufactured to circumvent the concern of heterogeneity in alignment and pores in laminar scaffolds for chondrocyte preservation and differentiation of stem cells in the bone marrow. With the objective of engineering bone lamellae, the alignment and osteogenic differentiation of MSCs on patterned *B. mori* silk films have been documented. Interestingly, for bone tissue engineering, good compressive strength (~13 MPa in hydrated state) 3D scaffold based on *B.mori* silk protein-protein interfacial bonding has been produced. Three layered wedge shaped *B. mori* silk scaffold system has been utilized for knee meniscus grafts. In addition, RGD-coupled, porous, patterned, mechanically sturdy and transparent *B.mori* silk films were made to imitate the architecture and hierarchy of corneal stromal tissue. Previous research also bears witness to the successful implementation of biocompatible *B.mori* fibroin / gelatin multilayer films to control the release of various compounds including trypan blue, FITC-inulin and FITC-BSA. In the meantime, For wound healing applications in skin tissue engineering, the prospects of mixing silk fibroin and human hair-derived keratin have been documented recently. On the other side, *Antheraea* and *Philosamia*, the *saturniid* silkworms, are two major sources of wild/non-mulberry silk in India. These silk varieties are symbolic of India's various serizons ' dynamic and rich cultural heritage. Citing for evidence, the splendor and picturesque floral motifs of a pair of muga (golden yellow silk, capped with the Geographical Indication, GI status) *mekhela chadar* (a traditional dress worn by Assamese women) reverberate the creative genius of the weavers and the work of the Assam state

sericulturists. It would be appropriate to mention at this juncture that research has been carried out at different research centers around the world on various non-mulberry silk biomaterials. Among other issues, initiatives are also underway to explore North-East Indian silk-based biomaterials using innovative approaches like those of electrospinning and others for tissue regeneration. These biomaterials can be used not only in tissue engineering, but also as models for 3D tissue disease and cell and drug delivery.

### **THE TYPICAL LIFE CYCLE OF AN INDIAN TASAR SILKWORM**

Wild or semi-domesticated silkworms show variations in the life cycle in terms of various parameters of physiology, morphology and feeding. For example, the life cycle of non-mulberry silkworms consists of four stages, i.e. Egg, larvae, pupae and adult stages (Figure 1). Life cycle duration also varies depending on the species of silkworm and climatic conditions (seasons).

- **Eggs**

The adult female moth lays fertilized eggs on the surface of the host plants leaves or in their vicinity under favorable conditions after copulation.

- **Larvae**

Larvae begin to eat and grow when the eggs have hatched. In the larval stages, all insects undergo various molting phases. The interval between different molts is termed as instar. Wild silkworms are tetra-molters that traverse five larval stages. The duration of the subsequent larval instars varies from 4 to 15 days, and the molting periods varies from 24 to 36 hours. The larvae stop feeding in the final stage; shorten their body size and begin to spin to form cocoon.

- **Pupae**

The larvae spin around a outer cover and this shell is called the cocoon. The pupation is occurring inside the cocoon. Larvae remain in the cocoon until moths of adults appear. The cocoon is spun in such a way that even under adverse conditions, the pupa remains well protected.

- **Adults**

After the condition becomes favorable, the pupa releases cocoonase, an enzyme that softens the cocoon for the moth to emerge, after emergence, the adult undergoes copulation and then lays eggs for the next generation to start.

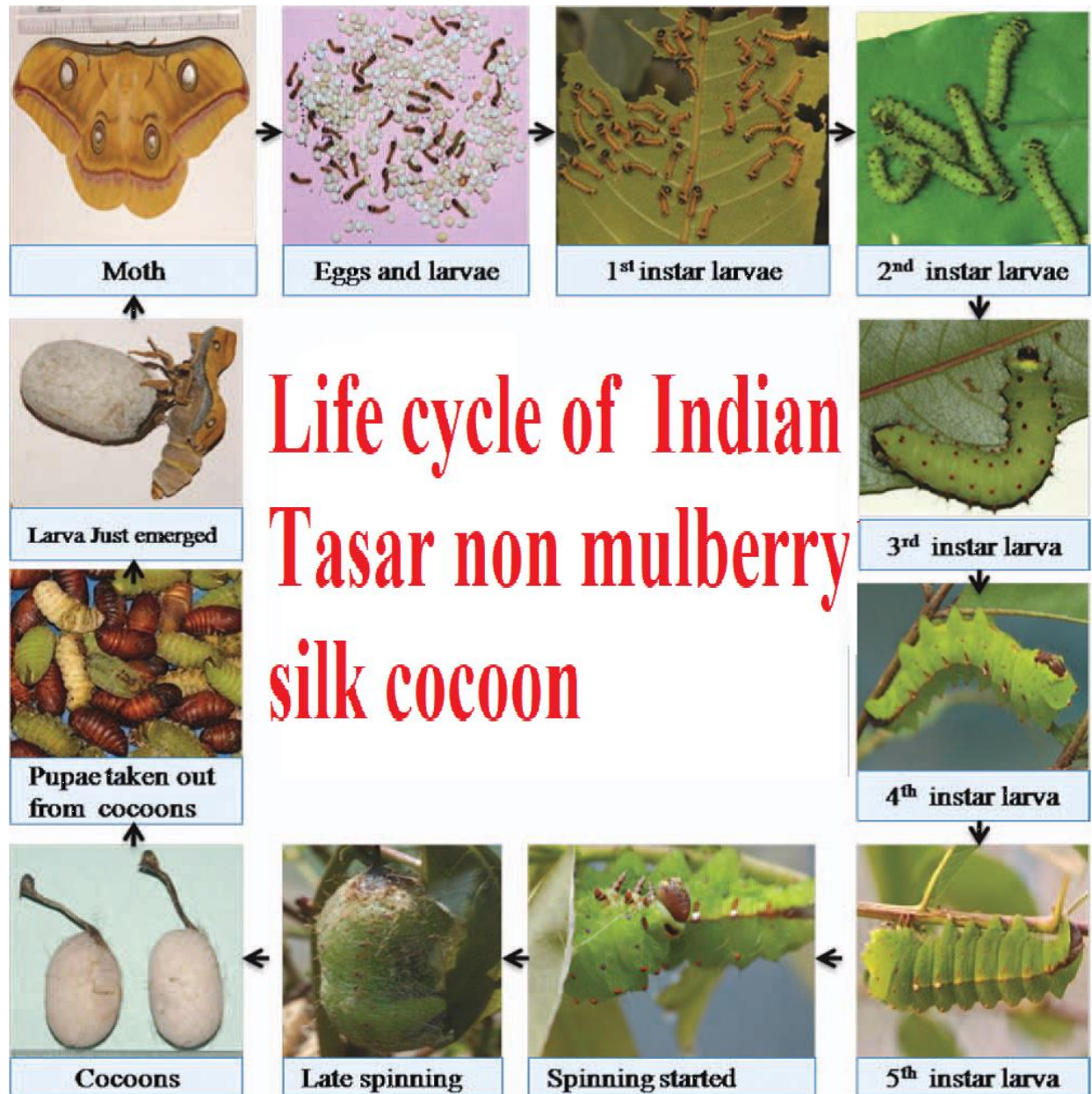


**FIGURE 1: TYPICAL LIFE CYLCE/DIFFERENT STAGES OF NONMULBEERY INDIAN TROPICAL TASAR SILKWORM, ANTHERAEA MYLITTA**

## **SILK PROTEINS**

Silk are protein polymers that are spread through several arthropods into fibers [7] and consist primarily of fibroin and sericin protein. Fibroin contributes to the toughness of the silk while sericin forms the cocoon and represents about 25–30 percent of the total cocoon weight (in the case of *B. mori*). Tasar silkworm has the highest capacity for silk production among all silk-spinning insects.[8] Cocoon construction of nonmulberry silkworms differs from cocoons of both mulberry and other members of the same nonmulberry silkworm family. The cocoons of *B.mori* has 10 layers whereas the tropical tasar (*A. mylitta*) cocoons has three distinct layers[8]–[10]. The properties of the silks obtained from each layer vary in the case of *B.mori*, while the silk obtained from the silkworms of the Saturniidae family exhibits similar characteristics[8]. The non-mulberry silkworm cocoons has a peduncle-like ring-like structure that attaches it to the tree and also serves as a sericin reservoir for the survival of natural obstacles and environmental hazard (Figure 2).[11] These peduncle which acts as a sericin reservoir for nonmulberry silkworms[11] and are absent in mulberry cocoons.



**FIGURE 2:** The cocoon of wild Indian tropical nonmulberry silkworm, *Antheraea mylitta* attached to twig of host plant with the help of peduncle (in the form of a ring to hold the tree branches), which is spun first.

The biological properties and functions of silk fibroin and sericin proteins are discussed in the following sections:

- **Fibroin**

It is the core structural protein of silk cocoons. Easy processing, biocompatibility, biodegradability, and high tensile strength of fibroin is make it gain attention in bio-medical applications. The features of fibroin, that makes it's a good option for tissue engineering purposes are enumerated below:



- Pure silk proteins obtained from mulberry and nonmulberry silkworms can be easily available.
- Isolation of fibroin from cocoons involves easy and less complicated process in case of mulberry only.
- Different morphological forms for example, powders, gels, films, hydrogels, 3D matrices, micro and nano-particles has been produced with relative ease from silk fibroin solutions.
- Silk proteins turns insoluble when immersed in an alcohol solution. This induces  $\beta$ -sheets formation, which facilitates to the development of silk fibroin-based biomaterials.
- Highly reactive sites in the amorphous region like basic amino acid residues enable modifications such as conjugation with lactose or blending with other polymers.
- Sericin which is a waste product from textile industries, has now found new ways into biomedical applications.

Mulberry silk fibroin's biocompatibility and mechanical properties have made it a worthy candidate for biomedical use. [2] The mechanical superiority of the silk is determined by the molecular structure, the water content, and the fiber formation process. The tensile strength of the silk fiber is determined by its  $\beta$ -sheet content. The  $\beta$ -sheets within the fibers are folded into highly ordered crystalline structures, resulting in strong hydrophobic interactions between the fibers and providing good strength to the fibers. The underlying nonmulberry silk (poly-Ala) polypeptide sequences are more hydrophobic than (poly-Gly-Ala), which is the most extensive sequence in mulberry silk. For poly-Ala  $\beta$ -sheets, it imparts a higher binding energy than poly-Gly-Ala  $\beta$ -sheets and contributes the relative difference in tensile strength between mulberry and nonmulberry. Table 1 portrays the tensile properties of silk cocoon fibers obtained from various species of silkworms.

**Table 1:** Molecular Weight and Tensile Strength of Silk Proteins (Fibroin and Sericin) Isolated from Different Mulberry and Nonmulberry Species[8]–[11]

<i>Types of silk</i>	<i>Silkworm Species</i>	<i>Silk Protein</i>	<i>Molecular Weights (kDa)</i>	<i>Extension (%) of Cocoon Fiber</i>	<i>Tensile Strength (GPa) of Cocoon Fiber</i>
<i>Mulberry silk</i>	B. mori	Fibroin	Three fractions obtained from gland; 350 kDa, 26 kDa, and 30 kDa. Two fractions obtained from cocoons; 325 kDa and 25 kDa	10.0–23.4	4.3 6 5.2
		Sericin	Gland sericin contains five polypeptides ranges from 80 to 310 kDa. Cocoon sericin exhibits polypeptides of 400 kDa, 250 kDa, 150 kDa and 24 kDa		
<i>Nonmulberry silk</i>	A. mylitta	Fibroin	Gland fibroin reported 395 kDa, and 197 kDa	26–39	2.5–4.5
		Sericin	Gland sericin give 5 different fractions ranging from 30 kDa to more than 200 kDa Cocoon sericin possess three fractions 70 kDa, 200 kDa and more than 200 kDa		
	A. assama	Fibroin	Two fractions of 220 kDa and 20 kDa	4–7	
		Sericin	Single fraction of 66 kDa		
P. ricini	Fibroin	Two fractions of 97 kDa and 45 kDa	24–28	1.9–3.5	
	Sericin	Single fraction of 66 kDa			

B.mori fibroin has been investigated extensively, both biochemically and biophysically. Silk proteins have relatively high molecular weight as summarized in Table 1. A bisulfide linkages links the heavy chain (H-fibroin) of B.mori's silk fibroin to a light chain (L-fibroin)[12] Glycoprotein, P25 operates as a chaperone and affects both H-fibroin transport and secretion. The main difference between the Bombycidae and Saturniidae members is the ratio (6:6:1) in which Bombycidae assembles H-fibroin, L-fibroin, and P25. L-fibroin and P25 are lacking in

Saturniidae[12]. other differences are the size of the non-repetitive C-terminus, H-fibroin repetitive sequences, and RGD tri-peptide motif. H-fibroin repetitive sequences are mostly hydrophobic in *B.mori*, whereas in the case of members of Saturniidae (*A.pernyi*) it is an modification of hydrophilic and hydrophobic. RGD (Arg-Gly-Asp) may be a justification to use them as a biomaterial.[12] Integrin, the molecule of the cell surface, binds RGD sequences., the presence of RGD sequences in nonmulberry silk i.e. *A.pernyi*, *A.yamamai* and *A.mylitta* [13] is beneficial over mulberry silk. Even in the presence of human lysozyme, integrin binding sequences continue elevated activity. RGD is lacking in Mulberry silk fibroin. The enactment of RGD motifs into mulberry silk fibroin matrices outcome in improved cell adhesion and proliferation. In addition, nonmulberry silk's wild nature makes it relatively easy to cultivate. Worldwide availability results in the culturally diverse distribution of different species of nonmulberry silks. The heterogeneous nature of various silks delivers the versatility to non-mulberry silk biomaterials. Due to the above-mentioned properties of non-mulberry silk, especially *A. Mylitta*, is receiving consideration in research areas. Silk fibroin also exhibits properties i.e. biocompatibility, superior strength, toughness and elasticity. *A. mylitta* silk fibroin can be developed into 3D scaffolds and 2D films for in vitro tumor modeling of multiple cancer types,skin, bone,[14] adipose, and drug delivery.

## **Sericin**

Sericin, the second major silk protein after fibroin, is 25–30% of the total weight of the mulberry cocoon. Mulberry sericin's molecular weight ranges from 20 to 400 kDa (Table 1 summarized). It does have a high amino acid content of serine (40 %), glycine (16 %), glutamic acid, aspartic acid, threonin, and tyrosine. Nonmulberry sericin is heterogeneous in nature and contains a peduncle sericin (200 kDa) in *A.mylitta*. *A.assama* and *Philosamia ricini* nonmulberry sericins are found to be biochemically and immunologically different from mulberry silk sericin.

Mulberry silk protein sericin has several unique properties that are useful for biomedical applications including antibacterial, antioxidant, antiapoptotic, antityrosinase, tumor suppressant, anticoagulant and wound healing.Sericin which has low molecular weight (~20 kDa) is used in cosmetics, food additives and in the pharmaceutical industry. while sericin with higher molecular

weight has been used as wound dressing, biodegradable biomaterials. *A. mylitta* nonmulberry sericin is similar to mulberry sericin and possess antioxidant properties. Pure, blended films and nonmulberry sericin scaffolds have already been produced and examined successfully as biomaterials. This *B. mori* and *A. mylitta* glue protein has the ability to form self-assembled nano and microstructures, which have hierarchical self-similar character across length scales in the form of a diffusion-limited, fractal assembly.

## **PROPERTIES OF SILK FIBRES**

### **Physical properties:**

- Silk fibers produced by the *Bombyx mori* silkworm are found to have a triangular cross section with rounded corners, 5-10  $\mu\text{m}$  wide. The fibroin-heavy chain is consist of mostly of beta-sheets, due to a 59-mer amino acid repeat sequence with a bit different variations. The flat surfaces of the fibrils has been found to reflect light at many angles, providing a natural shine to silk. The cross-section of other silkworms may vary in diameter and shape: for *Anaphe* as a crescent and for tussah as an elongated wedge. Silkworm fibers are naturally extruded as a pair of primary filaments (brin) from two silkworm glands, which are pinned together to form a bave with sericin proteins acting like glue. Tussah silk bave diameters can reach upto 65 $\mu\text{m}$ . [8]
- Silk has a smooth, soft texture which is not slippery, unlike many synthetic fibers.
- Silk has been found to be one of the strongest natural fibers but it loses up to 20% of its strength when it get wet. It has been found that silk has a good moisture regain of 11%. Its elasticity is moderate to poor: if elongated even a small amount, it seems to remains stretched. It get weakened if exposed to too much sunlight. It can also subjected to be attacked by insects, especially if left dirty.
- Silk has been found to be a poor conductor of electricity which makes it susceptible to static cling.
- Unwashed silk chiffon may shrink by up to 8 percent due to fiber macrostructure relaxation, so either silk should be washed prior to the construction of the garment or it should be dry cleaned. Dry cleaning can still reduce the chiffon by up to 4 %. occasionally, a gentle steaming with a press cloth can reverse this shrinkage. Due to molecular-level deformation, there is almost no gradual shrinking or shrinking.

- probably due to its molecular structure, Natural and synthetic silk has been found to manifest piezoelectric properties in their proteins.[8]
- Silkworm silk had been used as the standard for the denier which is a measurement of linear density in fibers. Silkworm silk therefore has a linear density of approximately 1 den, or 1.1 dtex.

### **Chemical Properties**

- Silk produced by the silkworm comprises of two main proteins, fibroin and sericin, fibroin being the structural center of the silk, and sericin being the sticky material surrounding it. Fibroin is made up of the amino acids Gly- Ser-Gly-Ala-Gly-Ala and forms beta pleated sheets. Hydrogen bonds forms in between chains, and side chains form above and below the plane of the hydrogen bond network.
- The high proportion (50%) of glycine, which is a small amino acid, allows tight packing and the fibers are strong and resistant to breaking. The tensile strength is due to the many interceded hydrogen bonds, and when stretched the force is applied to these numerous bonds and they do not break.
- Silk is resistant to most mineral acids, except for sulfuric acid, which dissolves it. It is yellowed by perspiration.

### **PROCESSING OF SILK PROTEINS**

Native silk obtained from silkworms demands regeneration of silk fibroin and removal of sericin before being fabricated into diverse biomaterial morphologies. A simple alkaline removal process is employed to remove sericin after harvesting cocoons. The degumming of *B.mori* results the highest yield of silk fibroin fibers, while the same process gives a lower sericin yield when applied to nonmulberry cocoons of *A. pernyi*, *A. mylitta*, and *Samia cynthia ricini*. The dissolution of nonmulberry silk cocoon is a formidable task. This is due to the presence of hydrogen bonding and the hydrophobic nature of fibroin. Silk glands of mature silkworm acts as an alternative source of silk proteins in nonmulberry. Silk fibroin is not just “squeezed out” of the silk glands but successfully solubilized and stabilized in 1% anionic surfactant (sodium dodecyl sulfate). The amount of silk protein fibroin obtained from the silk gland of a single silkworm is reasonably

better to process into a large numbers of 3D scaffolding matrices. The amount of protein obtained from a gland depends upon the crops and the season. For example *A. mylitta* relatively provides higher amount of fibroin from the last crop (i.e., the crop from winter season). Compared with *A. mylitta* (which produces three crops in a year), *A. assamensis* (that breeds five to six times in a year) provides less quantity of fibroin per mature larvae. Despite silk gland being used as a protein source from nonmulberry silkworms, there still is a serious demand of a suitable process to dissolve nonmulberry cocoons. Molecular weight determination of *A. mylitta* silk fibroin by SDS–PAGE electrophoresis shows single band of 395 kDa under nonreducing and 197 kDa under reducing conditions suggesting homodimeric nature of the protein.<sup>80</sup> No degradation of protein obtained from silk gland was observed as trail bands in electrophoresis suggests the retention of overall primary conformation of the protein obtained from gland. Band patterns of protein were similar to the fibroins extracted from cocoons using LiBr and LiSCN methods.[5] Depending on the requirement silk the silk fibroin solution can be easily processed from morphologies that range right from nano to the macroscale. The fabricated materials are given a 70% alcohol treatment to induce stability.[15] This treatment changes the mechanical behavior of the materials. Nonbioengineered silk fibroin protein obtained from silk glands are no different from silk proteins obtained from cocoons and are compared for cell culture in case of mulberry silks. Aqueous solution of lithium thiocyanate is strategically used for the dissolving nonmulberry silk fibroin of *A. pernyi*, *A. assama*, *P. ricini*, and *A. yamamai*. In response to this treatment, *A. pernyi* fibroin reveals a temperature sensitive sol–gel transformation. It also changes its molecular confirmation from random coil to  $\beta$ -sheet. This increases the stability of the matrix. Additionally the regenerated film of *A. yamamai*, initially consisting of  $\alpha$ -helix and random coil, induces  $\beta$ -sheet on being subjected to an ethanol treatment. This upgrades water resistance of the film.

## **NONMULBERRY SILK PROTEINS AS BIOMATERIALS**

The versatile nature of silk proteins makes silk-based materials an excellent candidate for biomedical applications. In this article, we specifically focus on the recent progress in research employing nonmulberry silk protein matrices for biomedical and biotechnological applications.

## **1. Tissue Engineering Scaffolds**

Pure silk fibroin scaffolds of *A. mylitta* have been reported to be successful in bone tissue engineering using human and rat bone marrow stem cells (BMSCs),[14] adipose tissue engineering using rat BMSCs[14] and cartilage tissue engineering using bovine chondrocytes. Besides freeze-dried scaffolds of *A. mylitta*, 3D silk fibroin scaffolds with reinforced ultrafine silk fibroin particles of *B. mori*, *Philosamia cynthia ricini*, and *A. assama* promotes osteogenesis of hBMSCs. Similar cell-compatible noncytotoxic results have also been obtained when the nonwoven 3D silk fibroin scaffolds of *A. assama* and *A. pernyi* 2D films are used. Scaffold of *A. assama* on sulfonation and has become more bio-reactive with human lung carcinoma cells . Besides tissue engineering, composites matrices of *A. mylitta* fibroin with polyethylene glycol (PEG-4000), hydroxypropylmethylcellulose- polyethylene glycol (HPMC-PEG) and *A. mylitta* sericin with gelatin or polyvinyl blend have exhibited cell compatibility. Blended electrospun nanofibrous scaffolds of polyvinyl alcohol and *A. pernyi* silk fibroin is biocompatible and seems to be an attractive alternative for tendon tissue engineering.

## **2. Tumor Modeling Matrices**

Studying molecular and genetic mechanisms underlying cancer initiation and progression using cancer cells in monolayer in vitro is a must for cancer research. However the 2D approach fails to mimic the native in situ tumor microenvironment and leads to distorted cell-integrin interactions.[17] Therefore attempt have been made to mimic 3D tumor microenvironment by utilizing *A. mylitta* fibroin scaffold. Prostate cancer cell line (LNCaP cells) and Human breast cancer cell line and in combination with 2D and 3D silk fibroin matrices have been compared in vitro. Yield coefficients of glucose consumption to lactic acid produced by cancer cells on *A. mylitta* silk fibroin scaffolds were found to be similar to that of cancer cells in vivo. Thus it may act as a tool for determining the efficiency of anticancer drugs.

## **3. Micromolded Devices and Self-Assembled Structures**

Micropatterning is used for monitoring cells, subcellular interactions and time-related changes of a cell due to various external agents including growth factors in a confined micro chamber. Silk

fibroin of *A. mylitta* is employed to fabricate micropatterned chambers. [18] The study has demonstrated cell-supportive nature of the nonmulberry fibroin grooved patterns, which can be commercialized further. Sericin's ability to form self-assembled nano and microstructures with hierarchical self-similarity across length scales in the form of a diffusion-limited fractal assembly helps in understanding its biological relevance in the formation of silk.

#### **4. Delivery Vehicles**

Self-assembly and mechanical toughness of nonmulberry silk are exploited to fabricate sustainable delivery vehicles of bioactive molecules in the form of nanoparticles and calcium alginate beaded-3D scaffolds.[19] Silk nanoparticles are prepared from silk fibroin solutions of *Antheraea mylitta*, measures 150–170 nm in average diameter and exhibit mostly Silk II structure. Cellular uptake studies have shown the accumulation of fluorescent isothiocyanate conjugated silk nanoparticles in the cytosol of carcinomic murine squamous cells. In-vitro VEGF release from the nanoparticles have demonstrated a sustained release over 3 weeks, signifying its potential application as a growth factor delivery system.

##### ➤ **Bio-nanocomposites**

BNCs have become a common term to designate nanocomposites involving a biopolymer in combination with an inorganic moiety, for example, layered silicate that shows at least one dimension on the nanometer scale [20]. These are the hybrid materials derived from natural polymers and inorganic materials interacting at the nanoscale. The BNCs can be prepared by using a variety of biopolymers and silicates. Till now, the inorganic solids such as layered silicates have drawn much attention of the biomedical industry. Their low cost, easy availability, relatively simple processing, and a considerable hike in the properties of the product make them a capable and efficient material [21]. These clays material are used as nanofillers in polymer composites [22]. Modification of clay leads to the intercalation of organophilic materials into the interlayer space of the clay which helps to weaken the interaction of interlayer of the clay that enhances the interlayer gap and upgrades the compatibility of clay-polymer. Due to this the macromolecules (proteins, drugs, DNA) are able to insert into the interlayer gap while processing, which causes



the separation of the discrete layers and consistent distribution of the Montmorillonite clay nanocomposites for drug delivery 637 individual layers of clay in a polymer matrix. These BNCs acquire several qualities such as mechanical strength, dimensional stability, low density, better surface area, etc [23]. Furthermore to these qualities, BNCs exhibit the outstanding benefits of showing biodegradability, biocompatibility, and functional properties due to the attachment of functional or biological moieties.

BNCs mainly formed of:

- Clay and clay minerals
- Biopolymers

- **Clay and clay minerals**

Clay is an inexpensive material that can be modified for a broad domain of applications by employing a number of methods such as ion exchange, acid treatment, metalmetal complex saturation, etc. In this context, it is worth to mention here that the nanoclay having a thickness of even less than 1 nm can be obtained by ion-exchange method.

**Table 2:** Major groups of clay minerals:

<i>S.no</i>	<i>Group name</i>	<i>Member minerals</i>	<i>General formula</i>	<i>Remarks</i>
1.	Kaolinite	Kaolinite, dickite, nacrite	$Al_2Si_2O_5(OH)_4$	Members are polymorphs (composing of the same formula and different Structure.)
2.	Smectite	Montmorillonite, pyrophyllite, talc, vermiculite, sauconite, saponite, nontronite	$(Ca, Na, H) (Al, Mg, Fe, Zn)_2 (Si, Al)_4O_{10}(OH)_2 \cdot XH_2O$	“X” indicates varying level of water in mineral type.
3.	Illite	Illite	$(K,H)Al_2(Si,Al)_4O_{10}(OH)_2 \cdot XH_2O$	“X” indicates varying level of water in mineral type.
4.	Chlorite	<b>i.</b> Amesite, <b>ii.</b> Chamosite, <b>iii.</b> Cookeite, <b>iv.</b> Nimite, and so on	<b>i.</b> $(Mg,Fe)_4Al_4Si_2O_{10}(OH)_8$ <b>ii.</b> $(Fe,Mg)_3Fe_3AlSi_3O_{10}(OH)_8$ <b>iii.</b> $LiAl_5Si_3O_{10}(OH)_8$ <b>iv.</b> $(Ni,Mg,Fe,Al)_6AlSi_3O_{10}(OH)_8$	Each member mineral has a distinctive formula. This group has fairly larger member minerals and sometimes considered as distinct group, not as part of clays.

The exceptional properties of nanoclay minerals are their low toxicity, biocompatibility, and hence considered as a potential candidate for controlled drug release [24], [25]. The nanoclays of great consideration are listed below:

- Hydrotalcite
- octasilicate
- Mica fluoride
- Montmorillonite (MMT)

The MMT is natural clay while the mica fluoride is synthetic one, whereas hydrotalcite and octasilicate have limited use. The MMT clays have an extensive range of use in polymers. It was found that MT could be supposed to be a good candidate for a number of applications.

- **Montmorillonite – a nanoclay**

Montmorillonite clay is natural nanoclay with a platy structure having a high internal surface area, good cation exchange capacity (CEC), efficient adsorption ability, and low toxicity [26]. MT clay has negatively charged layers with a fair enough swelling property in the presence of water. Due to which the positively charged substances get intercalated into the interlayer spaces via electrostatic interaction [27]. Several efforts have been made to form MT as a carrier for drug delivery that causes a controlled release of bioactive molecules [27]

- **Montmorillonite layered structure**

The components of cationic clay are octahedral and tetrahedral sheets known for the formation of nanohybrids. MMT categorizes into a group of phyllosilicates, its crystalline lattice composed of an aluminum-oxygen and aluminum hydroxyl octahedral sheet sandwiched by two silicon-oxygen tetrahedral sheets, which are frequently called medical clay. The layered structure is stacked together by van der Waal forces. This type of clay is known as 2:1 layer structure. The thickness of the layer is about 1 nm, and the other dimensions may vary from 100 to 1000 nm.

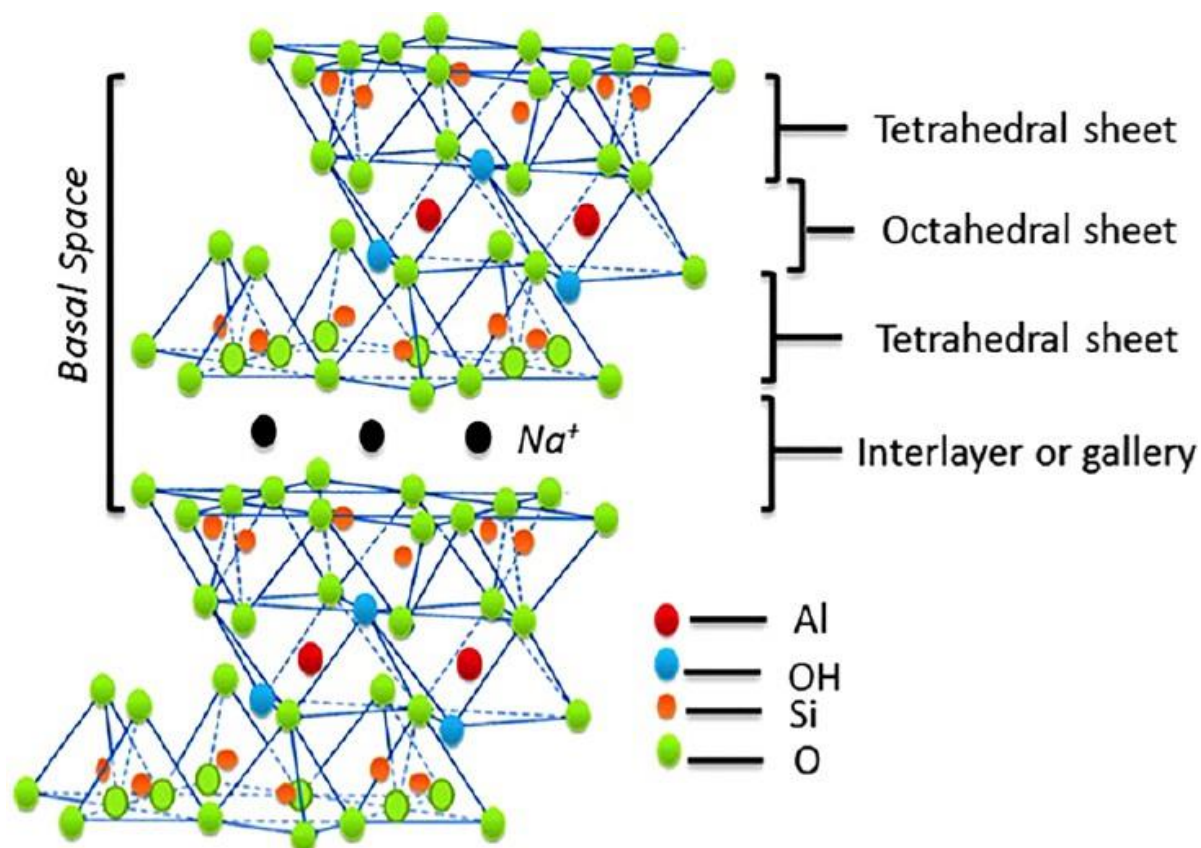


**Figure 3: Montmorillonite clay structure**

As discussed earlier, MMT has the swelling ability in presence of water cause hydration of interlayer cations[28]. The tetrahedral sheet consists of cations such as  $Si^{4+}$  and  $Al^{3+}$ , while octahedral sheet consists of  $Al^{3+}$ ,  $Fe^{3+}$ , and  $Mg^{2+}$ . Due to the isomorphic replacement of cations in both octahedral and tetrahedral sheets, the layered structure gets a permanent negative charge. The sodium ion can be replaced with organic cations, such as those from drug, dye, and biomolecules. The CEC of the clay can be characterized by the presence of negative charge of clay. The CEC of MMT is found in between 70 meq/ 100 g and 100 meq/100 g range. The X-ray d- spacing of dry  $Na^+$ - MMT is 0.96 nm and the thickness of platelet is around 0.94 nm [29]. But when sodium ion is exchanged for cationic drugs, biomolecules and polymers, the interlayer space increases and as a consequence X-ray d- spacing may multiply by twofold to threefold[29], while the thickness of MMT sheets remains same.

Clay has been successfully used as a nanoscale reinforcing phase for a wide range of commodity and natural polymers. Some natural polymer/clay materials with high-performance such as improved mechanical, thermal, and barrier properties have been achieved by several research groups. one of the obstacles in obtaining an excellent clay nanocomposite is the dispersion of the clay sheets in polymer matrix. Proteins are natural copolymers containing both hydrophobic and hydrophilic domains, which could interact with clay surface. Therefore, proteins could be used as excellent dispersants to clay. Because silk fibroin has potential use in the biomedical and composite industries, it is envisioned that incorporating clay platelets into silk fibroin would impart high tensile modulus and strength to the nanocomposites. This may open the gateway to produce multifunctional silk materials that may be used as tissue scaffold, artificial tissue, and biodegradable structural materials.

**Table 3:** Important physical properties of montmorillonite clay:

<i>S.NO.</i>	<i>PROPERTY NAME</i>	<i>DESCRIPTION</i>
1.	DENSITY	2–3 g/cm <sup>3</sup>
2.	CRYSTAL SYSTEM	Monoclinic
3.	HARDNESS	1–2 on Mohs scale, soft, possess fine-grained occurrence
4.	FRACTURE	Irregular, uneven
5.	CLEAVAGE	Perfect
6.	LUSTER	Earthy, dull
7.	TRANSPARENCY	Translucent
8.	COLOR	White, buff, yellow, green, rarely pale pink to red (presence of high valance Mn produces pink to red coloration)

➤ **Functional properties:**

• **Cation exchange property**

Cation exchange capacity is a property of soil introduced by clay and organic matters. It is the capacity of soil to hold cations (generally  $\text{Ca}^{2+}$ ,  $\text{Fe}^{2+}$ ,  $\text{Zn}^{2+}$ ,  $\text{Al}^{3+}$ ,  $\text{Mn}^{2+}$ ,  $\text{Cu}^{2+}$ ,  $\text{Na}^+$ ,  $\text{Mg}^{2+}$ ,  $\text{K}^+$ ,  $\text{H}^+$ ) and described as the quantity of positively charged ions held by the negatively charged surface of clay minerals. It may also be termed as cation exchange capacity (CEC) that may be measured as a centimol positive charge per kg of soil or milli-equivalent (meq) of positive charge per 100 g of soil.

Fine-grained particles of clay are found to have an increment in the surface area per unit mass. Smaller particle size (0.002–0.001 mm in diameter) which results in a considerably higher surface area, where a large number of cations are found to be adsorbed. These adsorbed cations can give significant level of electrical conductivity in clay.

Ionic substitution in the sheet structure produces useful modifications. Ions like  $\text{Fe}^{3+}$  and  $\text{Al}^{3+}$  are small enough to enter the tetrahedral coordination with oxygen and substitute  $\text{Si}^{4+}$ . Similarly, cations like  $\text{Mg}^{2+}$ ,  $\text{Fe}^{2+}$ ,  $\text{Fe}^{3+}$ ,  $\text{Li}^+$ ,  $\text{Ni}^{2+}$ , and  $\text{Cu}^{2+}$  can substitute  $\text{Al}^{3+}$  in the octahedral sheet. Large-sized cations such as  $\text{K}^+$ ,  $\text{Na}^+$ , and  $\text{Cs}^+$  are located between the layers and referred as interlayer cations.

• **Electrical conductivity**

Clay particles are the porous materials. The pore fluid influences the electrical conductivity. The electrical conductivity (mS/m) of a porous material is the combination of electrical conductivities of the matrix material and the pore fluid.

Air, water, or saline water may be present in the pore. When the pore fluid is of low conductivity, for example, air or water, the bulk conductivity of clay mineral is contributed by the matrix material. Pore fluid having a higher electrical conductivity significantly enhances the total electrical conductivity of clay, for example, clay particles with a significant porosity level (40–

50%), and saline water present in the pore; then the bulk conductivity is mainly the contribution of pore fluid. In this case, there would be negligible difference in the conductivities of sand and clay.

A higher content of clay particles with 2:1 structure present in montmorillonite sample produces an increased bulk electrical conductivity for non-saline soils. This effect was attributed to the exchangeable cations or to proton transfer from the dissociation of interlayer water content. A reduced level of interlayer water contents in K-saturated clays resulted in the lowest electrical conductivity.

Since the clay content, pore fluid, clay type, saline water, and water saturation influence the soil conductivity, the assessment of electrical conductivity of reservoir rock may be used to estimate these factors. However, the variation in the distribution of liquid and solid phases introduces the variation and complication in the electrical conductivity of heterogeneous porous medium.

The distribution of electrical ions around clay pores is called membrane polarization. In membrane polarization, the negative ions are oriented to one end of the pore under the influence of DC potential across the clay pore, and this polarization resists the current flow.

In the study of soil, the clay content in soil can be determined using electrical conductivity and membrane polarization as the function of clay content.

- **Water sorption**

Water sorption is an important characteristic of natural clay particles. Clay particles can absorb or lose water in response to changes in humidity content in the ambient environment; when water is absorbed, it fills the spaces between the stacked silicate layers.

Montmorillonite typically exhibits a gradual dehydration and phase change to a stronger nonexpandable clay. The specific gravity of any type of clay is variable resulting from loss or gain of water. Most of the known clay types are available in nature as a mixture containing several varieties including carbonates, feldspars, micas, and quartz.

Several studies addressed the swelling behavior of montmorillonite. The interaction of montmorillonite with water introduces useful effects. Water molecules cause swelling in montmorillonite. This swelling is a result of complex montmorillonite-water interactions between particles and within the particle itself.

Water molecule adsorption and swelling of montmorillonite introduce hydrated states and hysteresis. The migration of counter-ion, initially bound to montmorillonite surface to the central interlayer plane, leads to swelling in montmorillonite. Therefore, charge locus in montmorillonite has a strong influence on swelling dynamics.

An important concern in clay mineral study is how the monovalent and divalent cations affect the swelling pattern of  $K^+$ ,  $Na^+$ , and  $Ca^{2+}$ -montmorillonites.

Montmorillonite is a 2:1 clay mineral; that is, two tetrahedral sheets separated by one octahedral sheet. The montmorillonite platelets can be negatively charged when:

- tetrahedral substitution of Si by Al in two tetrahedral sheets, or
- octahedral substitution of Al by Mg in central octahedral sheet.

In any of the above two cases, negative charge produced is compensated by interlayer ions. The hydration of interlayer cations seems to produce swelling[30].

The small platelet size and stacking structure has been found as complicated to precisely characterize through experiment. Therefore, molecular dynamic simulation (MDS) is a useful technique of understanding the atomic level structure. MDS has been found useful in the study of montmorillonite structure including swelling and hydration of interlayer cations. MDS was performed for  $K^+$ ,  $Na^+$ , and  $Ca^{2+}$ -montmorillonites with different ranging level of water content.

The valence of the cations showed a significant influence on montmorillonite-water system. Simulations indicate that the cation  $K^+$  shows a strong interaction with dehydrated montmorillonite sheets; however, in case of hydrated montmorillonite sheets, cation  $Ca^{2+}$  interacts



strongly. Therefore, the layer spacing of simulated  $K^+$ -,  $Na^+$ -, and  $Ca^{2+}$ -montmorillonites was obvious.

The concurrent measurement of swelling and swelling pressure was done utilizing a researcher-developed cell [30]. Undisturbed clay samples at a defined swelling (0–75%) had been removed from the cell and analyzed using different techniques for e.g. SEM, FTIR, and ATR (micro-attenuated total reflectance) spectroscopy. Silicate (Si-o)-stretching region ( $1150\text{--}950\text{ cm}^{-1}$ ) showed significant changes with variation in swelling and orientation. It was found that the reduced particle size with increased swelling was related to increased misorientation of the clay platelets. The rearrangement of clay platelets was observed as a direct result of the breakdown of the clay particles with increased hydration.

### ➤ **Functional utilization**

The addition of montmorillonite in material, polymer, and products may result in significant enhancement in the required performance. Interestingly, there is a great variety of montmorillonite utilization as an additive in composite or as a functional filler in polymers. The results obtained indicated useful effects. Examples included the applications as food additive for health and stamina, for antibacterial activity, as sorbent for nonionic, anionic, and cationic dyes, and as catalyst in organic synthesis, and so on.

- **Montmorillonite in biopolymer**

Biopolymer modification using montmorillonite as nanofiller is found to improve the thermo-mechanical properties. Biopolymer produced from chitosan/montmorillonite nanocomposite through diluted acetic acid used as solvent for dissolving and dispersing chitosan and montmorillonite.

Pure chitosan was compared with chitosan-montmorillonite nanocomposite with and without acetic acid in terms of morphological structure and selected properties. Results obtained in XRD

and TEM showed an intercalated and exfoliated nanostructure at a reduced montmorillonite loading and an intercalated and flocculated nanostructure at an increased montmorillonite loading.

Thermal stability and mechanical properties were determined using TGA and nanoindentation. Thermal stability, hardness, and elastic modulus of nanocomposite matrix improve with the increasing loading of nano-dispersed montmorillonite. Crystallinity, thermal stability, and mechanical properties may be influenced by acetic acid residue in chitosan matrix.

The study of montmorillonite in potato starch showed the improvement in thermal and Young modulus properties. Nanocomposite films of glycerol-plasticized starch/ montmorillonite were produced. Three different loadings of montmorillonite aqueous suspension were applied to potato starch.

Dispersion of montmorillonite in starch was studied using X-ray diffraction (XRD). Results indicated that the nanomontmorillonite formed an intercalated structure and complete exfoliation was not observed under the experimental conditions used. Thermogravimetric analysis indicated the enhancement in the thermal resistance with the increased loading of montmorillonite; however, the water absorption by the starch-montmorillonite nanocomposite, at 75% constant relative humidity, was reduced. The result of micro-tensile test of nanocomposite film showed that Young modulus improved up to 500% at 5 wt.% of montmorillonite .

- **Drug delivery system**

Adsorption and swelling characteristics of montmorillonite are useful in drug delivery systems. An increased adsorption capacity provides improved drug entrapment and sustained release of pharmaceutical drugs. Solubility, dissolution rate, adsorption, and bioavailability of hydrophobic drugs are enhanced by montmorillonite. The effects of montmorillonite in improving the drug delivery system were reviewed[31].

- **Adsorption of dyestuff**

Effluent loading, from dyeing industries and textile-processing units, to natural environment is a serious concern. Technological solution is required to remove residual dye content from the used water. The application of montmorillonite as an adsorbent for cationic dye is an important effect. The removal of cationic dye, methylene blue, from water is achievable through adsorption process. Montmorillonite concentration used for the removal of cationic dye depends upon the initial dye concentration, contact time, solution pH, and temperature. Results obtained on dye adsorption demonstrated the equilibrium data follow the Langmuir isotherm equation.

Thermodynamic study of methylene blue adsorption on montmorillonite indicates that the process is endothermic revealed by the determination of enthalpy, entropy, and Gibb's free energy. Importantly, the results support the possibility of using montmorillonite as low-cost adsorbent for wastewater treatment containing cationic dyestuff. There is a large number of textile dyeing industries, in India, Pakistan, and China, that release used dye bath water containing cationic dyestuff. Adsorption system developed using montmorillonite can be useful for water recycling in dyeing industries.

Possibly, montmorillonite can be used to influence the optical, chemical, and spectral characteristics of cationic dyes. The layer charge of montmorillonite can affect the cationic dye molecular aggregation. The subject was reviewed through the research literature discussing dye reaction with clay minerals[32].

- **Adsorption of toxic heavy metals**

An important application of adsorption properties of montmorillonite is seen in the removal of toxic heavy metals from aqueous solution. The adsorption studies using montmorillonite and kaolinite for the removal of toxic metals including As, Cd, Cr, Co, Cu, Fe, Pb, Mn, Ni, and Zn were reviewed. Montmorillonite and its modified forms exhibited a significantly increased metal adsorption capacity relative to kaolinite and modified kaolinite. The modified clay mineral form was produced by pillaring montmorillonite or kaolinite by using polyoxy cations including  $Zn^{4+}$ ,

$\text{Al}^{3+}$ ,  $\text{Si}^{4+}$ ,  $\text{Ti}^{4+}$ ,  $\text{Fe}^{3+}$ ,  $\text{Cr}^{3+}$ , or  $\text{Ga}^{3+}$ . The modified form can also be produced using quaternary ammonium cations including tetramethylammonium-, tetramethylphosphonium-, and trimethylphosphonium-,  $\text{N}^-$ -didodecyl-N,  $\text{N}^-$ -tetramethylethanediammonium, etc.

Montmorillonite modified using sodium dodecylsulfate (SDS) can remove  $\text{Cu}^{2+}$  and  $\text{Zn}^{2+}$  by sorption from aqueous solutions. The study was conducted as a function of solution pH, solute concentration, and temperature (25–55°C). The thermodynamic parameters ( $\Delta H^\circ$  and  $\Delta S^\circ$ ) for  $\text{Cu}^{2+}$  and  $\text{Zn}^{2+}$  sorption on modified montmorillonite were evaluated. The study finds out that the kinetics for the sorption of  $\text{Cu}^{2+}$  and  $\text{Zn}^{2+}$  was assessed and the pseudo-first-order rate constant was evaluated.

### **III. EXPERIMENTAL WORK**

#### **1. Materials:**

Multivoltine silk cocoons of Tasar silkworm *Antheraea mylitta* were procured from Silk Development Department, Sonbhadra, Uttar Pradesh, India. 1-butyl-3-methylimidazolium acetate (BMIMAc) and gentamicin sulphate were purchased from Sigma-Aldrich, India. Reagent grade of sodiumbicarbonate for degumming process, silver nitrate, copper chloride and quarternary ammonium salt (Benzalkonium chloride) for modification of montmorillonite nanoclay were procured from Sigma Aldrich. Montmorillonite nanoclay were purchased from SRL.

#### **2. Modification of the sodium-montmorillonite clay with Copper chloride, silver nitrate and benzalkonium chloride.**

Initially 3g of Na-MMT clay was weighed and 50ml of 1mM solution of copper chloride was prepared and then 3g clay is mixed into beaker containing 30ml of above solution with continuous stirring for 7 days at temperature 37°C. after 7days, the solution is dried in the oven at 60°C for two days and then the clay agglomerate are crushed using mortar-pistar to make the clay particles uniform in size. Same procedure is followed for the modification of Na-MMT clay by silver nitrate and benzalkonium chloride salts.

#### **3. Extraction of the tasar silk fibroin from tasar *antheraea mylitta* cocoons**

Degumming of the tasar silk fibroin from the tasar silk cocoon was done firstly by cutting the tasar silk cocoons into small pieces and then boiling it in the Na<sub>2</sub>CO<sub>3</sub> solution for one hour and the silk fibroin is filtered and sericin is collected in a jar for future use. Silk fibroin extracted was washed several times to remove the small tarces of sericin present in it and dried at 60°C.

#### **4. Preparation of silk fibroin solution**

Dissolution of silk fibroin in the ionic liquid was performed in the two-neck round bottom flask with nitrogen atmosphere. Briefly, degummed tasar silk fibroin fibers were dissolved in ionic liquid (1-butyl-3-methylimidazolium acetate) at 100-120 °C in the concentration of 10% (w/v)

under nitrogen atmosphere. Tasar silk fibroin fibers dissolved completely in BMIMAc within 2h under nitrogen atmosphere on constant stirring. After dissolution, the solution is filtered through mesh.

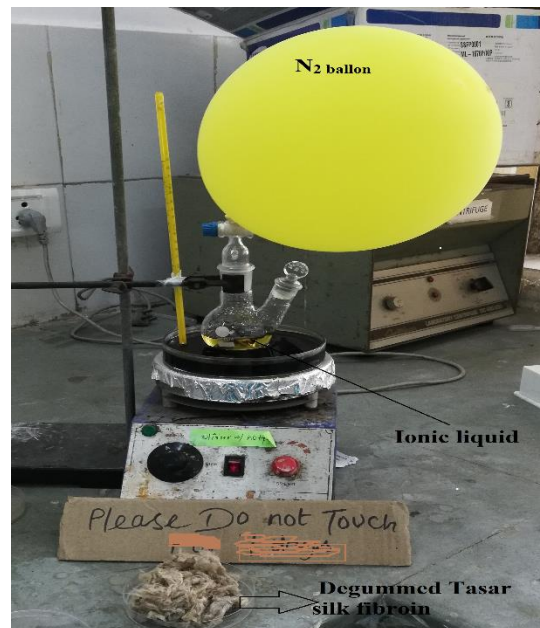


**Figure 4 : Dissolution of degummed tasar silk fibroin in ionic liquid with continuous stirring**

### **5. Preparation of silk fibroin/bioactive clay film by solution casting**

Tasar silk fibroin-BMIMAc solution (10% w/v) was prepared by dissolving 5g of silk fibroin into 50ml of ionic liquid at temperature of 100-110°C with continuous stirring in two neck round bottom flask till the homogenous solution is obtained. Then 2.5mg, 5mg, and 25mg of different modified clay was added each time to 5ml of above homogenous solution to prepare 0.5%, 1%, and 5% (w/w) solution with ultra-sonication for uniform dispersion of clay particles in the solution. Then it was poured into polystyrene Petri plates to prepare films of thickness ( $0.50 \pm 0.1$  mm).

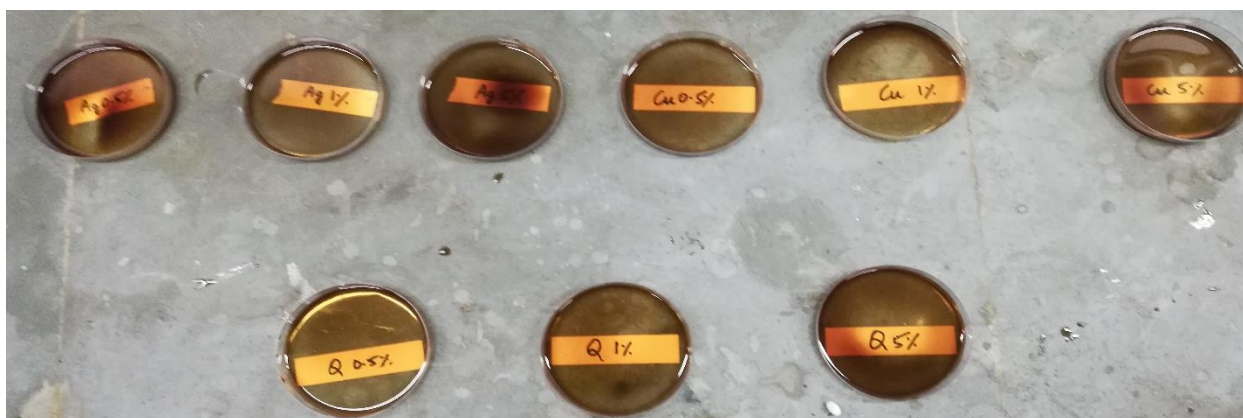


**Figure 5: preparation of tasar silk fibroin/bioactive clay nanocomposite films**

After 2 h, methanol was added to each plate and was allowed to crystallize for 5 h. The ionic liquid was removed from film samples as reported by Silva *et al.* [116].

## **6. CHARACTERISATION METHODS:**

### **a) Fourier transform infrared spectroscopy**

Structural conformation of different Tasar silk fibroin/bioactive clay nanocomposite films was determined by Thermo Scientific Nicolet 380 Spectrometer, Japan, in reflection mode at  $4\text{ cm}^{-1}$  resolution using 64 scans in the spectral range  $4000$  to  $400\text{ cm}^{-1}$ .

### **b) Morphological and elemental characterization**

Different samples of modified bioactive clays were sputter coated with gold and analyzed by Field Emission Electron Microscope with EDS (JEOL Model JSM-7900F Prime with Oxford-EDS system IE 250 X Max 150) at an accelerating voltage of 5 kV with the magnification level from 5000x up to 100000x. Elemental analysis of modified clay was done using EDX..

### **c) Particle size analysis**

Mean particle size and volume fraction of the nanoparticles were measured in the milliQ water, using Particle Size Analyzer (Microtrac S 3500).

### **d) TEM**

For TEM, a drop of the sonicated aqueous suspension of nanocomposite powder in ethanol was drop cast on carbon coated copper and mounted at the JEM-1400 Transmission Electron Microscope (TEM) & then analyzed at the voltage of 120kV and magnification upto 6000- 30,000x.

### e) Thermal analysis

The thermogravimetric analysis (TGA) measurement of different tasar silk fibroin/bioactive clay nanocomposite film samples were performed on a Perkin Elmer Diamond TGA instrument. The amount of sample was approximately 5 mg. All the measurements were performed under nitrogen atmosphere from 30 to 900 °C at a heating rate of 10°C/min.



### f) Structural characterization of different regenerated tasar silk fibroin/bioactive clay nanocomposite film constructs by XRD

The X-ray scans of different films constructs as well as different types of modified mmt clay were performed with a Seimens type-F, X-ray diffractometer (Bruker D S Advanced, Germany). The X-ray source was Cu K $\alpha$  radiation (40 kV, 30 mA and  $\lambda=1.5$  Å). The samples were mounted on aluminum frames and scanned from 2 to 30° (2 $\theta$ ) at a speed of 2°/min.

### g) Antimicrobial activity test

The antimicrobial activity of tasar silk fibroin/ bioactive nanocomposite film samples was studied by broth dilution method against bacterias *E. coli* (gram -ve) and *S. aureus* (gram +ve). The tasar silk fibroin/ bioactive nanocompositefilm samples had been cut in the circular shape of diameter 10mm and sterilized in UV light under laminar air flow for time interval of 12 h. The sterile samples were put on agar plates which already had been cultured with *E. coli* and *S. aureus* and pressed a bit to assure the close contact with the film surface. The the plates were incubated at 37°C for 16 h in an incubator chamber. After incubation, sample were taken out and diluted with



the milliQ water and the again spread over culture medium and then the results has been evaluated by counting number of colonies formed around the sample during incubation period to assess the antimicrobial activity of tasar silk fibroin/ bioactive nanocomposite film samples.

#### **h) Minimum inhibitory concentration (MIC)**

Minimum inhibitory concentration of the treated montmorillonites was determined by the broth dilution method. Modified Montmorillonite powders were dried in an oven at 50°C for 2 h, weighted accordingly in a weighing balance to make solutions of different concentrations in test tubes with deionized water. A 2% solution of luria broth was prepared and 10ml of luria broth solution were taken separately in equal number of test tubes. After that 1ml of each test tube containing modified mmt clay solutions was put into every test tube containing broth solution and then test tubes containing both solutions(clay solutions and luria broth solution) were autoclaved for 1hour to eradicate all bacteria and then test tubes were put under laminar flow. After that each test tube is incorporated with 20 $\mu$ l of bacterial solution and incubated at 37°C for 16 hours. After 16 h, turbidity was checked in each test tube. Cell culture medium from agar-agar and luria broth solution was prepared. Then each turbid test tube was diluted five times. After dilution, 20 $\mu$ l solutions of each test tube was spread all over the culture medium and then medium plates were incubated at 37°C for next 16 hours. After incubation period, minimum inhibitory concentration was determined by counting the number of colonies formed in the culture medium. Finally, the plate with least number of colonies was found to be minimum inhibitory concentration value.

## IV. RESULT AND DISCUSSION:

### 1. THERMOGRAVIMETRIC ANALYSIS (TGA)

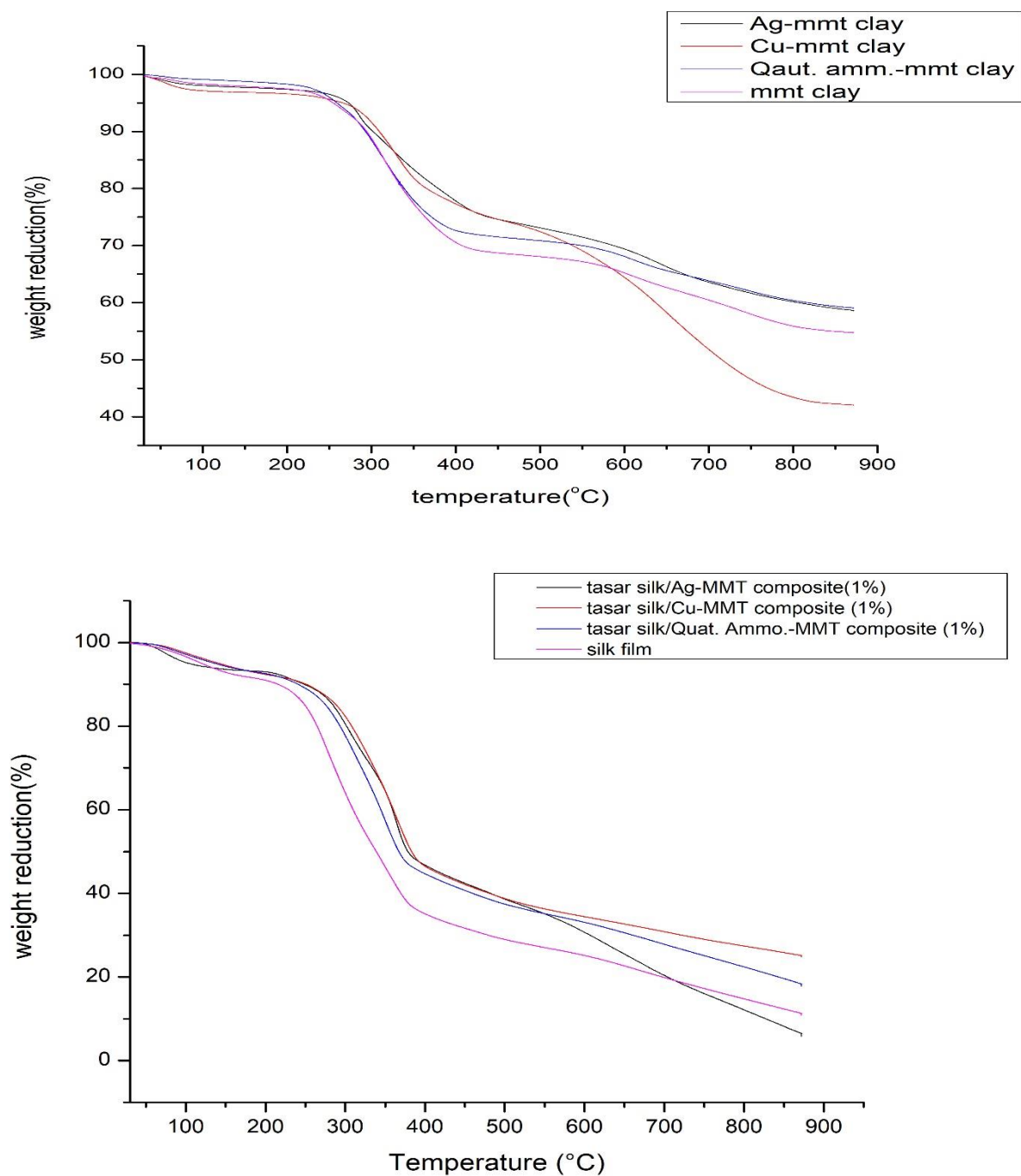


Figure 6: TGA of different modified mmt clay and tasar silk/bioactive clay nanocomposite films

TGA gives us information about the thermal stability of the modified clay. The TGA curves for unmodified Na-MMT clay and modified clays are shown. It is noted that the TGA of the unmodified montmorillonite has been categorized into three mass loss steps: Between ambient and 100°C, at 135°C and at 450°C. These mass loss steps are responsible for the desorption of water from the clay, dehydration of the hydrated cation in the interlayer and the dehydroxylation of the montmorillonite respectively. The presence of organic cation increase the number of decomposition steps. Four steps of the mass loss steps are observed for the modified clays [33]. In case of pure Na<sup>+</sup>-MMT clay , the first step is from the ambient to 66.9°C temperature range and is attributed to the desorption of water. The second step occurs from 135.5°C to 310°C and is assigned to the loss of hydration water from the Na<sup>+</sup> ion. The third mass loss step is attributed to the removal of the surfactant at around 440°C. The fourth mass loss step in the TGA curves is assigned to the loss of structural hydroxyl groups from within the clay. It is around 580°C. This shows that the thermal stability of modified MMT clay.

Further, the TGA curves of copper, silver and quaternary ammonium salt modified clay shows first degradation step from ambient to 50°C temperature range. The second step occurs from 245°C to 326°C and third step occurs at occurs at 560°C. The second and third decomposition steps are important for utility of such organically modified montmorillonites in high temperature applications. Pure silk film show first degradation at 80-100°C and second degradation at 300°C which got shift to 350°C after incorporation of modified clay which confirms the formation of nanocomposite films.

## **2. PARTICLE SIZE ANALYSIS:**

The particle size of the different modified mmt clay was found to be ranges from minimum size which is 225 nm to the maximum size which is 363nm.

**Table 4:** Particles size of different types of modified MMT clay

<i>S.NO.</i>	<i>MONTMORILLONITE CLAY</i>	<i>MEAN PARTICLE SIZE DIAMTER (nm)</i>
1.	Copper modified mmt clay	225
2.	Silver modified mmt clay	220
3.	Quarternary ammonium salt modified mmt clay	224

### **3. SEM and EDX:**

- **SILVER MODIFIED MMT-CLAY**

From SEM images, it was observed that the modified clays are composed of heterogeneous particles. The modified clay sample presented a layered flake morphology characteristic of clays, with particle size between 150 and 250 nm. Elemental chemical analysis by EDX was carried out in all the samples. After the ionic exchange, total Ag content 0.2 wt %, and Copper content 0.2 wt% and quaternary ammonium salt (0.1wt%) for the silver modified mmt-clay, copper modified mmt-clay sample and quaternary modified. all modified samples showed a diminution of Na<sup>+</sup> that Na<sup>+</sup> is preferentially exchangeable by Ag<sup>+</sup>, Cu<sup>2+</sup> therefore, the decrease in sodium content can content after ion exchange; the decrement was stronger in the ground sample. It have been found be associated with the incorporation of Ag<sup>+</sup>, Cu<sup>2+</sup>ons in the samples by cation exchange.

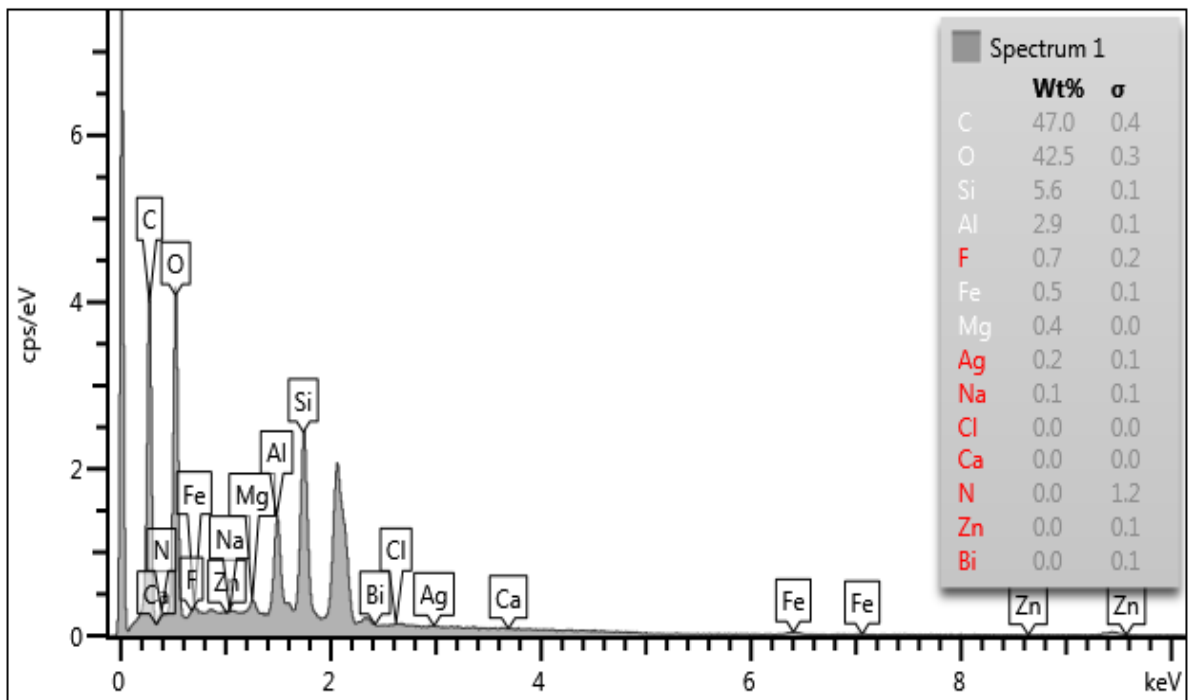
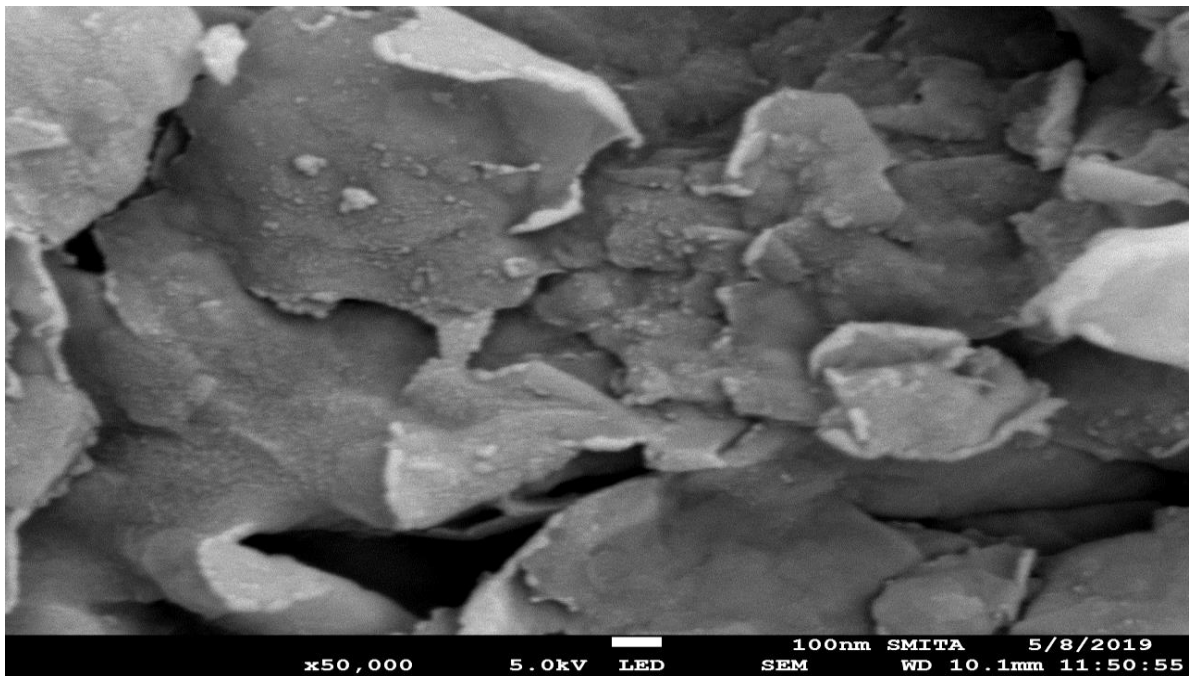
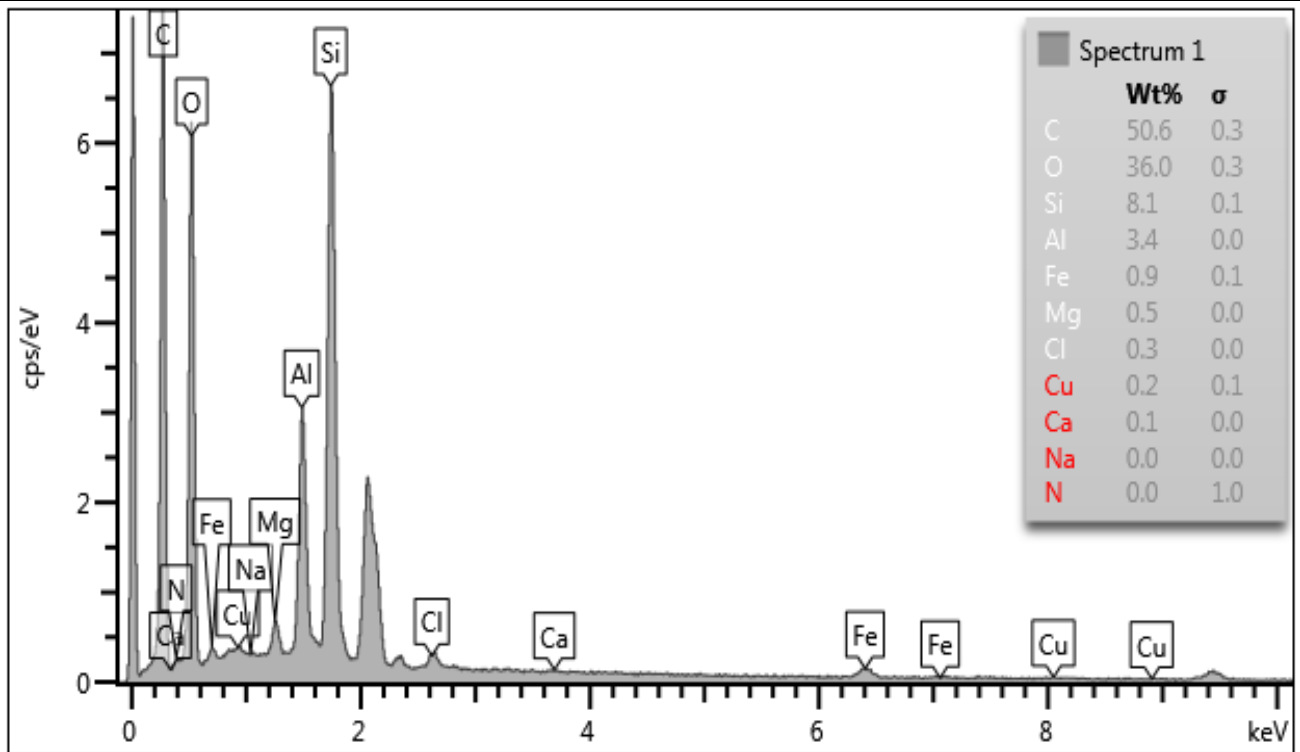
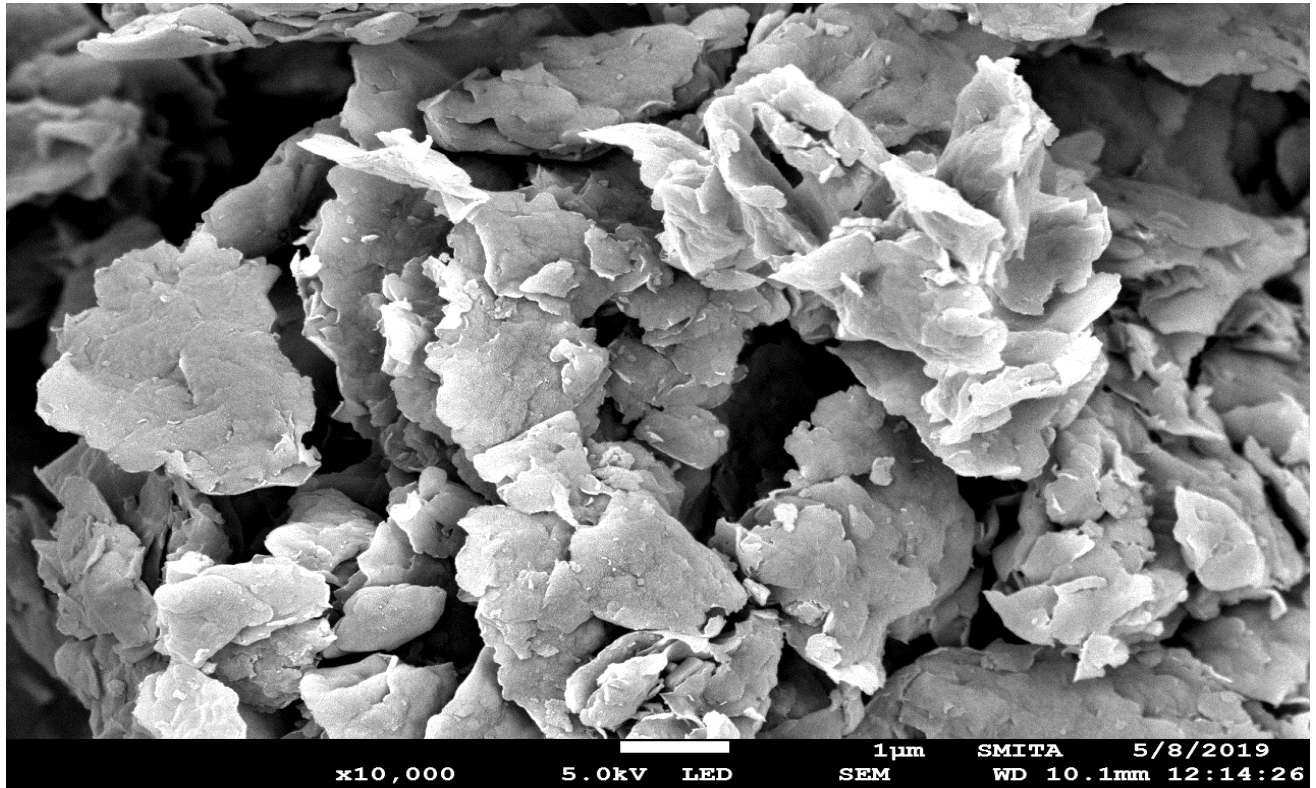


Figure 7: SEM and EDX of silver modified clay

- **COPPER MODIFIED MMT-CLAY:**



**Figure 8: SEM and EDX of copper modified clay**

- **QUARTERNARY AMMONIUM MODIFIED MMT-CLAY:**

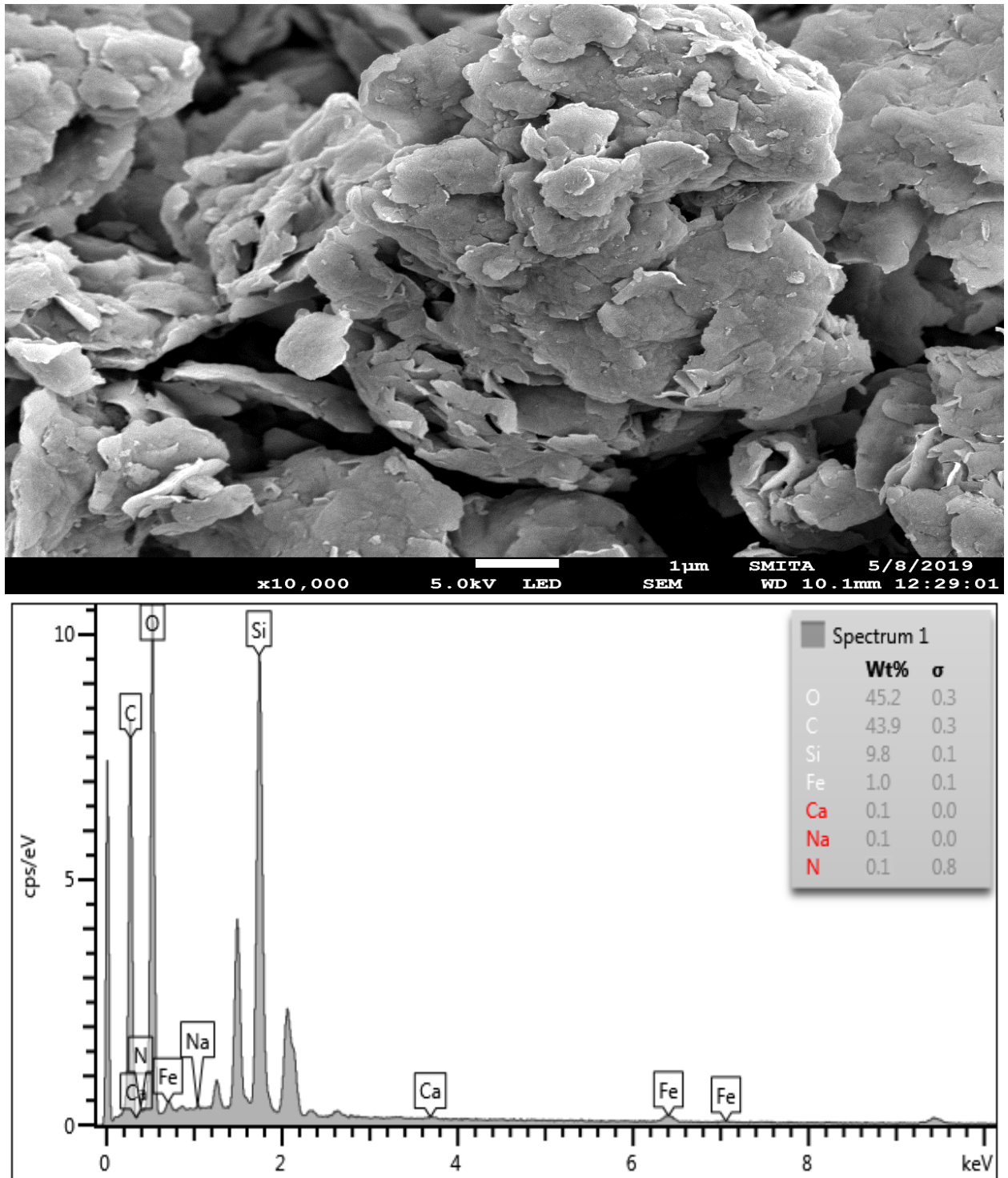


**Figure 9: SEM and EDX of Quat. Ammo. modified clay**

#### 4. TEM:

It has been found that in the tasar silk fibroin/bioactive clay nanocomposite films, due to reduction of silver, TEM images showed the presence of small black nanoparticles on the surface of clay flakes of the exchanged samples as it is reported earlier as After Ag modification, TEM images showed the presence of white nanoparticles on the surface of the exchanged samples, which are below 10 nm. While in other modified clay, reduction of copper or quaternary ammonium salt has not taken place and nanoparticles were not observed.

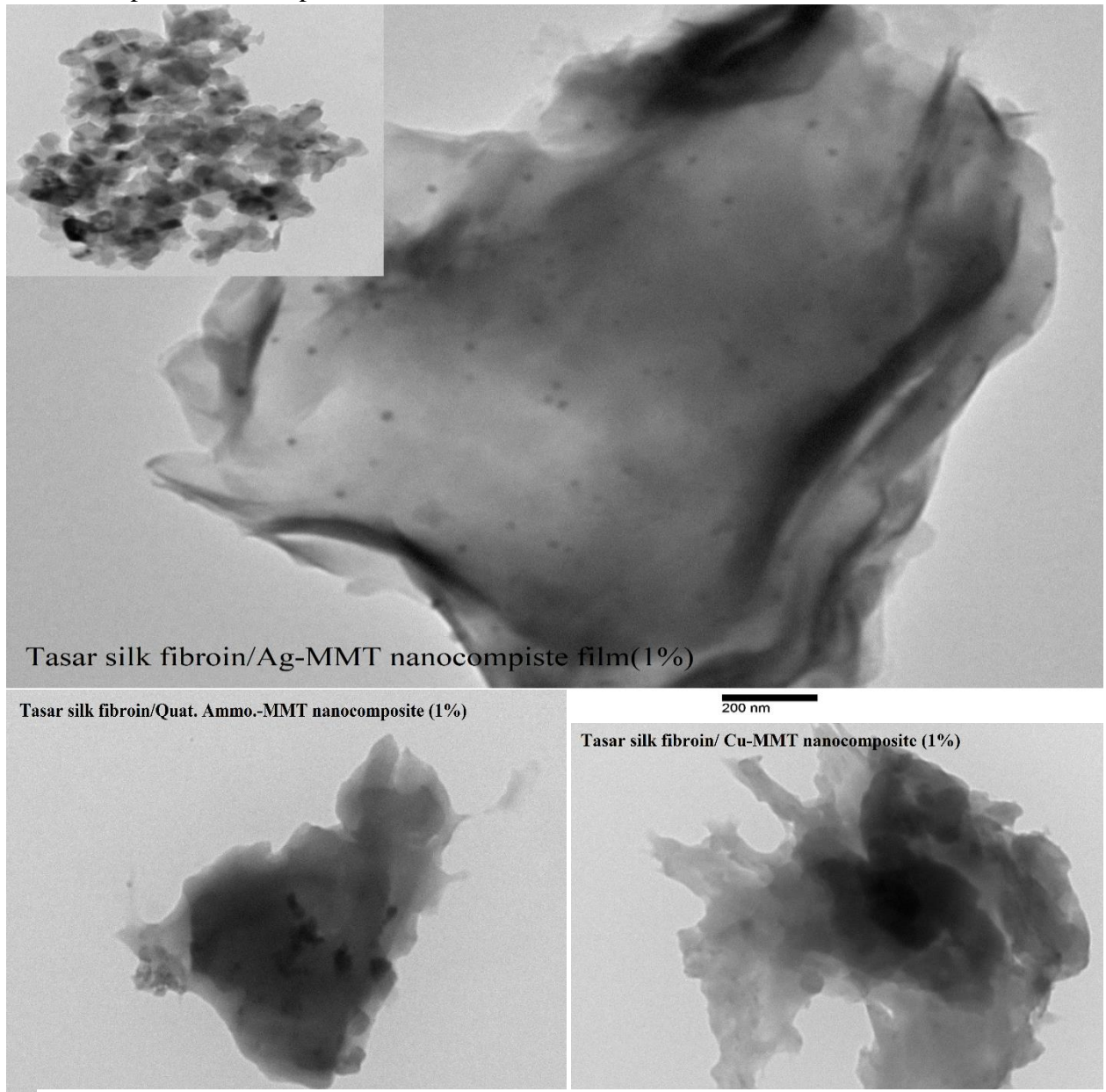


**Figure 10: TEM of tasar silk fibroin/ bioactive clay nanocomposite films**



## 5. FTIR

Tasar silk fibroin showed two broad absorption peaks with a center around  $1625\text{ cm}^{-1}$  (amide I) and  $1523\text{ cm}^{-1}$  (amide II), corresponding to silk II conformation ( $\beta$ -sheet). Tasar silk fibroin/bioactive clay nanocomposite treated with different concentrations of bioactive clays (0.5 to 5%) showed peaks of amide I and II regions. These are  $1631\text{ cm}^{-1}$  and  $1530\text{ cm}^{-1}$  for 0.1% nanocomposite film,  $1632$  and  $1531\text{ cm}^{-1}$  for 1% nanocomposite film,  $1633\text{ cm}^{-1}$  and  $1532\text{ cm}^{-1}$  for 5% nanocomposite film, which represents the characteristic of less ordered  $\beta$ -sheet conformation.[34]

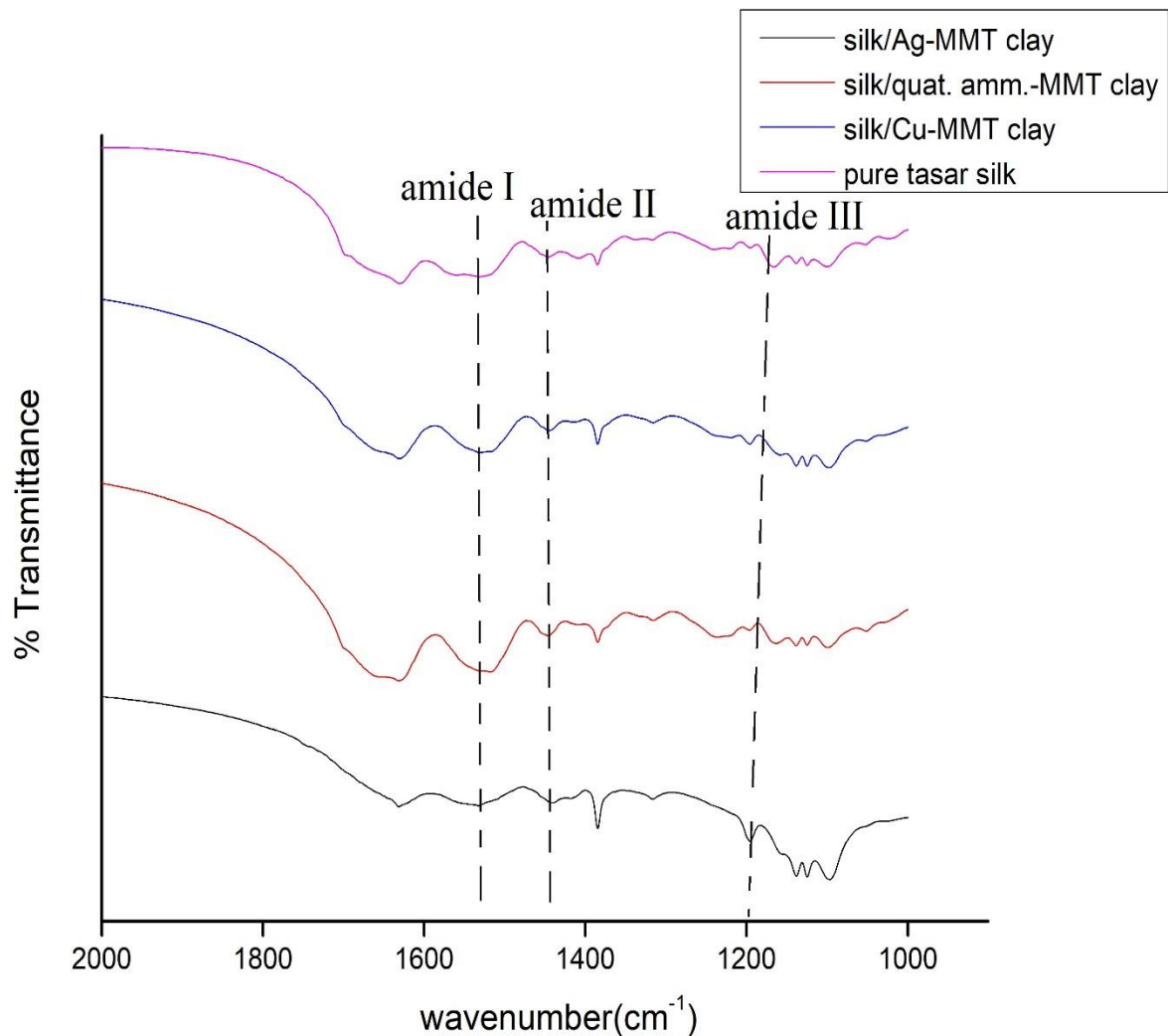


**Figure 11: FTIR of tasar silk fibroin/bioactive clay nanocomposite films**

## 6. ANTIBACTERIAL ACTIVITY:

- **Antimicrobial Activity**

Antimicrobial activity is one of the most essential requirements of biomaterials. The most satisfactory model correlated to antimicrobial activity of the modified clay is the interaction between positively charged clay molecules and negatively charged microbial cell membranes. Here, the antibacterial properties of different cations exchanged montmorillonites have been attributed to the attraction, by electrostatic forces, of the negatively charged membrane of the bacteria to the surface of the clay, where the positive charged metal ions kills the bacteria or renders them unable to replicate. The minimum inhibitory concentration (MIC) was found to be 0.42mg/ml and 0.67mg/ml for Cu-MMT clay against E.coli and S.aureus respectively (Table 5). The MIC was found to be 1.1mg/ml and 1.9mg/ml for Ag-MMT clay against E.coli and S.aureus respectively (Table 6). The MIC was found to be 3.9mg/ml and 5.3mg/ml for quat. Ammo.-MMT clay against E.coli and S.aureus respectively (Table 7). Tasar silk fibroin/MMT nanocomposite films with 1% weight percentage of different modified clay showed better antibacterial properties than other concentrations.

**Table 5: Antibacterial activity of Cu-MMT clay:**

S.NO.	Conc. of Cu-MMT (mg/ml)	Staphylococcus aureus		Escherichia coli	
		(CFU * 10 <sup>5</sup> /ml)	Antibacterial activity (%)	(CFU * 10 <sup>5</sup> /ml)	Antibacterial activity (%)
1.	CONTROL	500±2.5	--	700±3.8	--
2.	0.42	--	--	116±2.4	83.4±1.6
3.	0.43	--	--	220±3.7	68.5±2.2
4.	0.44	--	--	192±1.9	72.5±1.3
5.	0.65	15±1.6	97.0±1.2	--	--
6.	0.66	24±4.2	95.2±2.4	--	--
7.	0.67	13±4.1	97.4±3.1	--	--
8.	0.68	23±3.4	95.4±1.9	--	--
9.	0.69	27±2.6	94.6±1.3	--	--

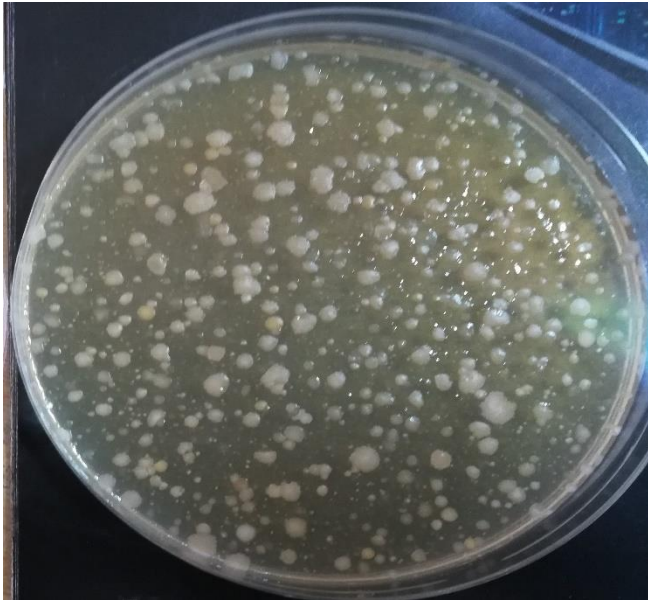
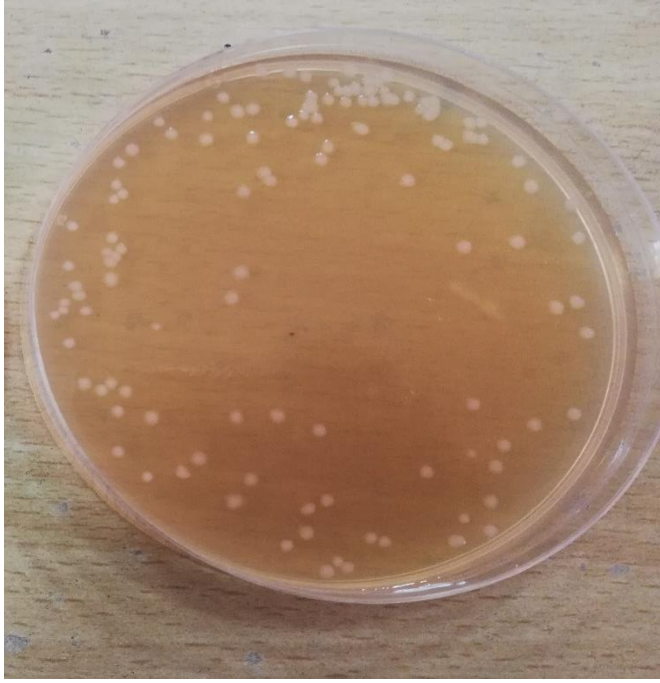


**Figure 12: microbial colonies formation during antibacterial testing**

**Table 6: Antibacterial activity of Ag-MMT clay:**

S.NO.	Conc. of Ag-MMT (mg/ml)	Staphylococcus aureus		Escherichia coli	
		(CFU * 10 <sup>5</sup> /ml)	Antibacterial activity (%)	(CFU * 10 <sup>5</sup> /ml)	Antibacterial activity (%)
1.	CONTROL	800±2.3	--	740±2.8	--
2.	0.9	--	--	125±3.3	83.1±1.6
3.	1.0	--	--	118±5.7	84.0±2.4
4.	1.1	--	--	104±6.8	85.9±3.8
5.	1.8	110±1.6	86.2±1.1	--	--
6.	1.9	78±3.4	90.2±1.2	--	--
7.	2.0	96±4.7	88.0±2.4	--	--

**Table 7: Antibacterial activity of Quat. Ammo.--MMT clay:**

S.NO.	Conc. of Quat.ammonium salt-MMT (mg/ml)	Staphylococcus aureus		Escherichia coli	
		(CFU * 10 <sup>5</sup> /ml)	Antibacterial Activity (%)	(CFU * 10 <sup>5</sup> /ml)	Antibacterial Activity (%)
1.	CONTROL	900±2.7	--	550±2.7	--
2.	3.8	--	--	39±1.6	92.9±1.1
3.	3.9	--	--	24±4.3	95.6±2.3
4.	4.0	--	--	52±4.8	90.5±3.1
5.	4.1	--	--	53±8.6	90.3±3.3
6.	4.2	--	--	56±4.1	89.8±1.8
7.	4.3	--	--	48±2.5	91.2±1.1
8.	4.8	222±1.6	75.3±1.2	--	--
9.	4.9	233±2.3	74.1±1.1	--	--
10.	5.0	237±4.5	73.6±2.6	--	--
11.	5.1	322±4.8	64.2±2.7	--	--
12.	5.2	220±7.6	75.5±3.3	--	--
13.	5.3	150±5.3	83.3±2.4	--	--

**Table 8: Antibacterial activity of Tasar silk fibroin/Ag—MMT nanocomposite film:**

S.NO.	TASAR SILK/ Ag-MMT NANOCOMPOSITE FILM	E.COLI (CFU * 10 <sup>5</sup> /ml)	<i>Antibacterial activity (%)</i>	S.AUREUS (CFU * 10 <sup>5</sup> /ml)	<i>Antibacterial activity (%)</i>
1.	CONTROL	1200	--	900	--
2.	1.0%	232±1.6	80.6±1.1	120±3.1	86.6±2.3
3.	5.0%	238±3.3	80.1±2.1	136±4.6	84.8±2.6

**Table 9: Antibacterial activity of Tasar silk fibroin/Cu—MMT nanocomposite film:**

S.NO.	TASAR SILK/ Cu-MMT NANOCOMPOSITE FILM	E.COLI (CFU * 10 <sup>5</sup> /ml)	<i>Antibacterial activity (%)</i>	S.AUREUS (CFU * 10 <sup>5</sup> /ml)	<i>Antibacterial activity (%)</i>
1.	CONTROL	1000	--	1000	--
2.	0.5%	527±2.1	47.3±1.6	154±5.6	84.6±3.3
3.	1.0%	150±3.2	85.0±2.1	147±4.6	85.3±3.1
4.	5.0%	288±1.8	71.2±1.2	169±3.8	83.1±2.1

**Table 10: Antibacterial activity of Tasar silk fibroin/Quat. Ammo.—MMT nanocomposite film:**

S.NO.	TASAR SILK/ QUAT. AMMO.-MMT NANOCOMPOSITE FILM	E.COLI (CFU * 10 <sup>5</sup> /ml)	<i>Antibacterial activity (%)</i>	S.AUREUS (CFU * 10 <sup>5</sup> /ml)	<i>Antibacterial activity (%)</i>
1.	CONTROL	1300	--	1000	--
2.	0.5%	258±2.3	80.1±1.2	223±4.5	77.7±2.3
3.	1.0%	339±3.4	73.9±1.6	170±3.6	83.0±1.5
4.	5.0%	294±1.8	77.3±1.0	245±2.1	75.5±1.1

## **7. X-RAY DIFFRACTION:**

In the below figures XRD patterns of pristine MMT and tasar silk/ bioactive clay composites has been demonstrated. The pristine MMT clay produced primary peak at  $2\Theta = 7.08^\circ$ . According to Bragg equation, the spacing of the pristine MMT has been calculated to be 1.25 nm. After the cation exchange, this peak got shifted to  $5.24^\circ$ , corresponding to a spacing of 1.66 nm, which is broader than that of pristine MMT. In the composite, this peak shifted to  $5.16^\circ$ , corresponding to a spacing of 1.675 nm, which is little more broader than that of pristine MMT.[35]

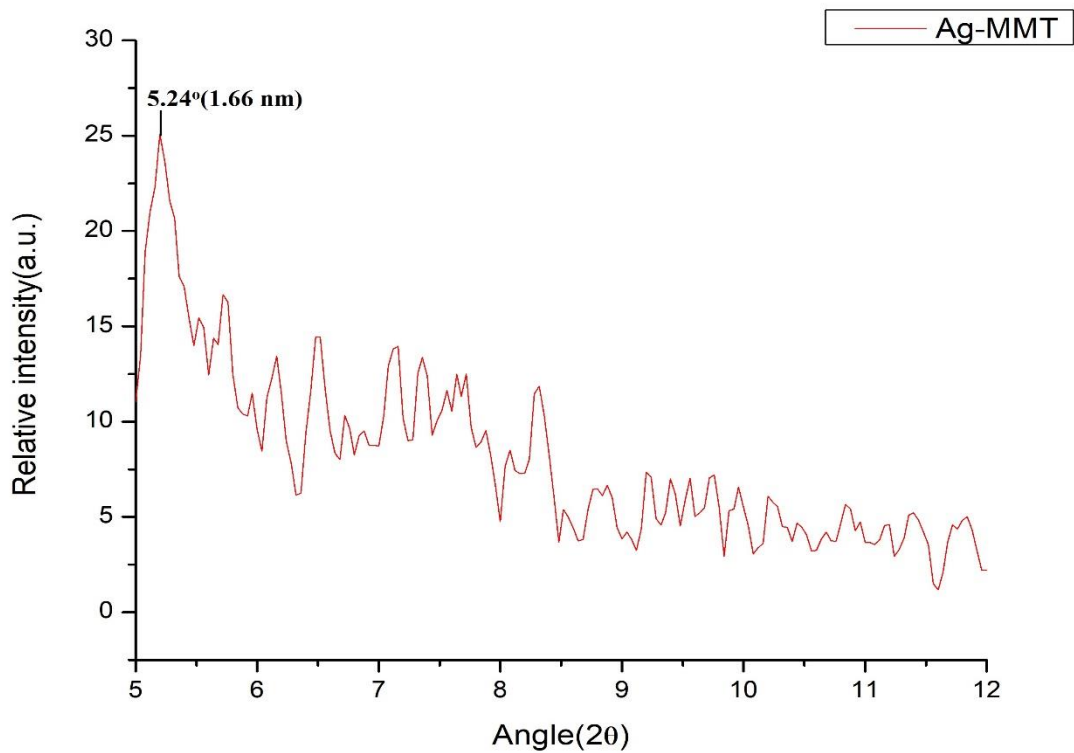
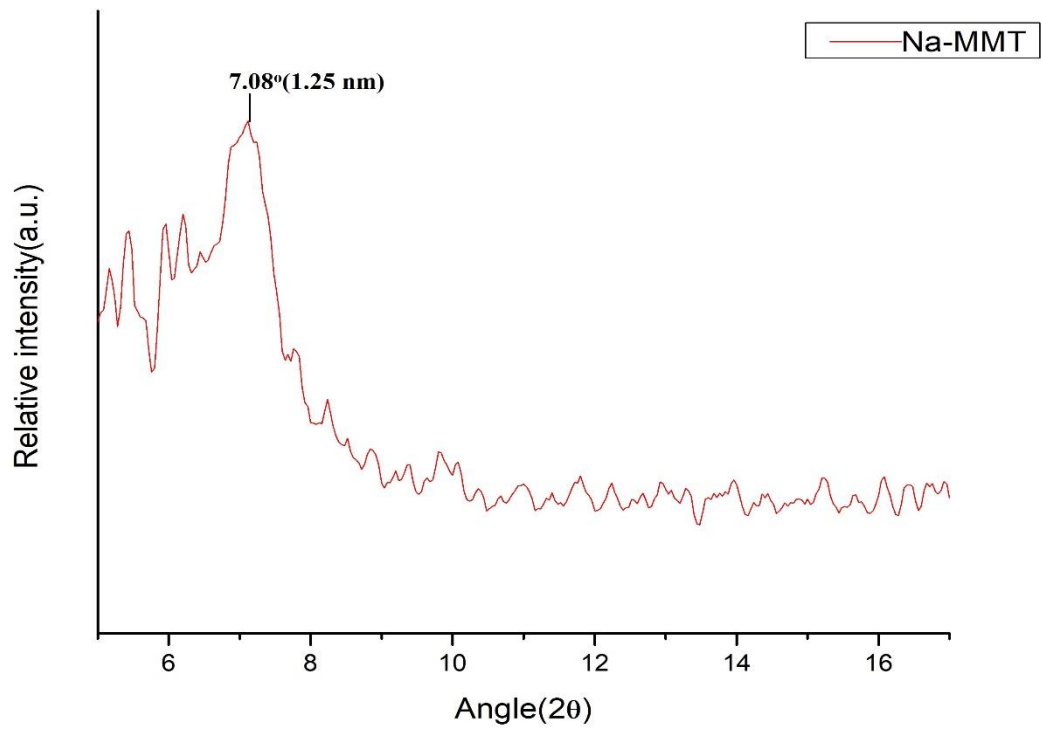


**Figure 13: XRD of pristine Na-MMT and Ag-MMT clay**

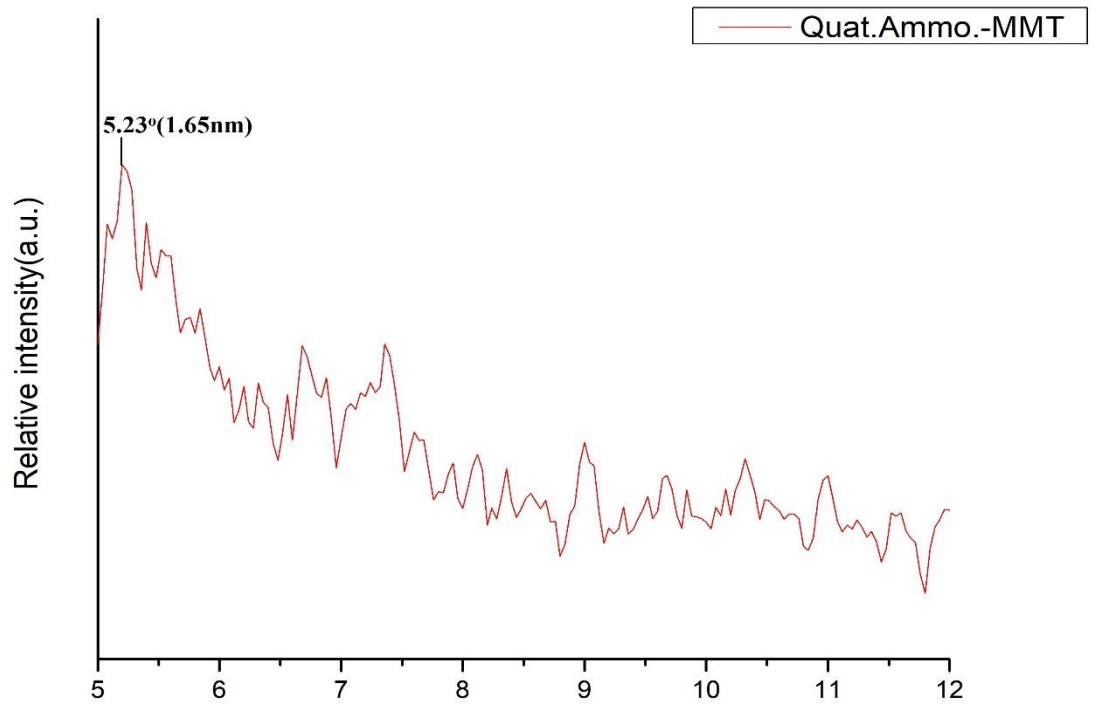
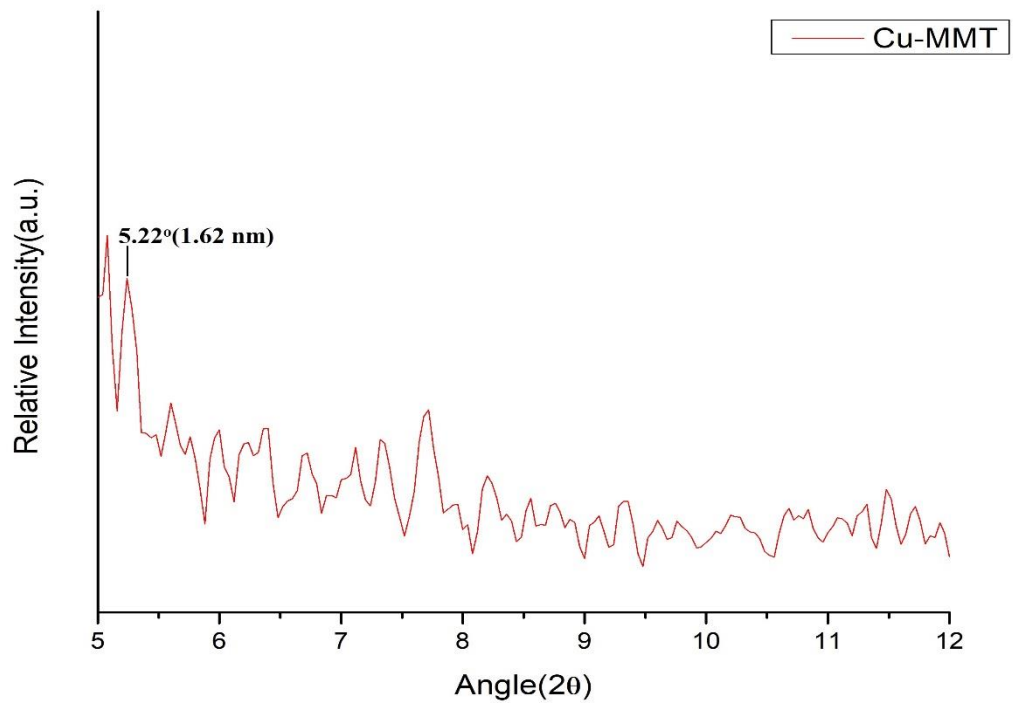


**Figure 14: XRD of pristine Cu-MMT and Quat. Ammo-MMT clay**

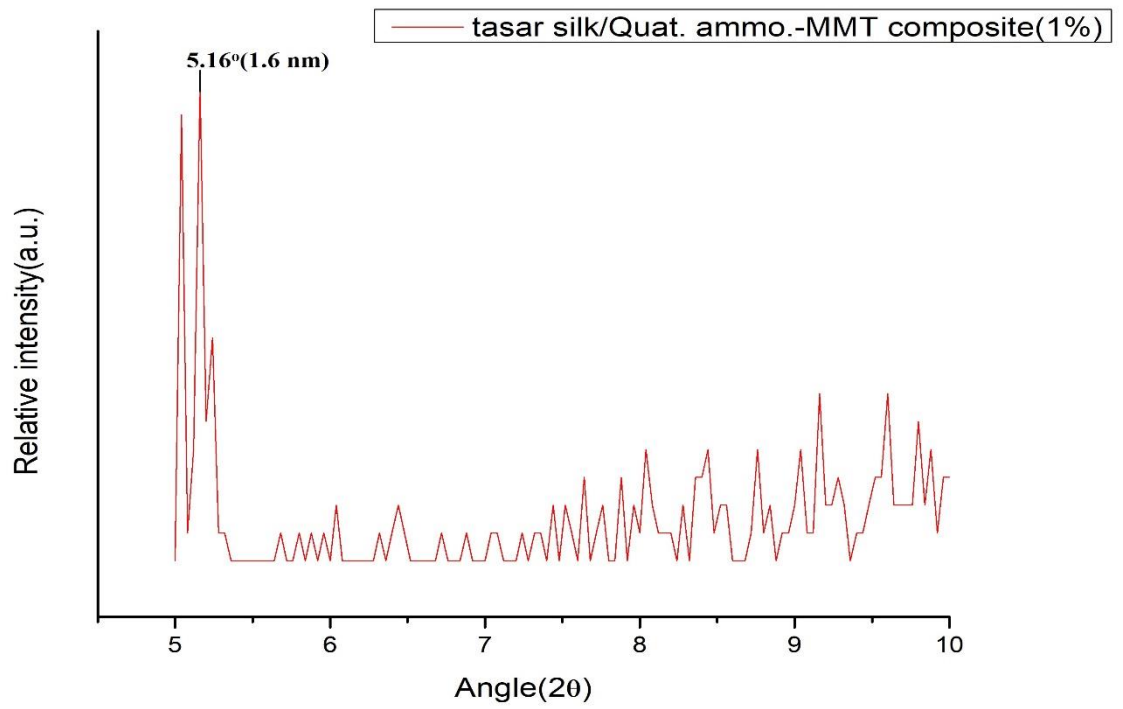
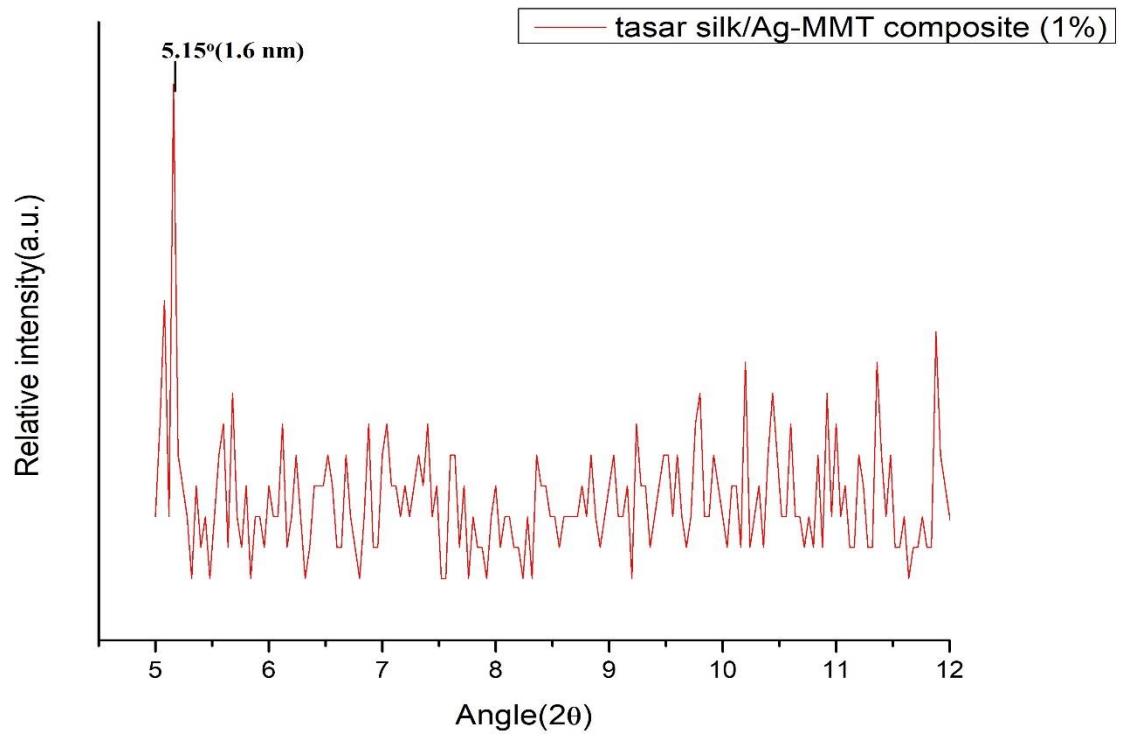
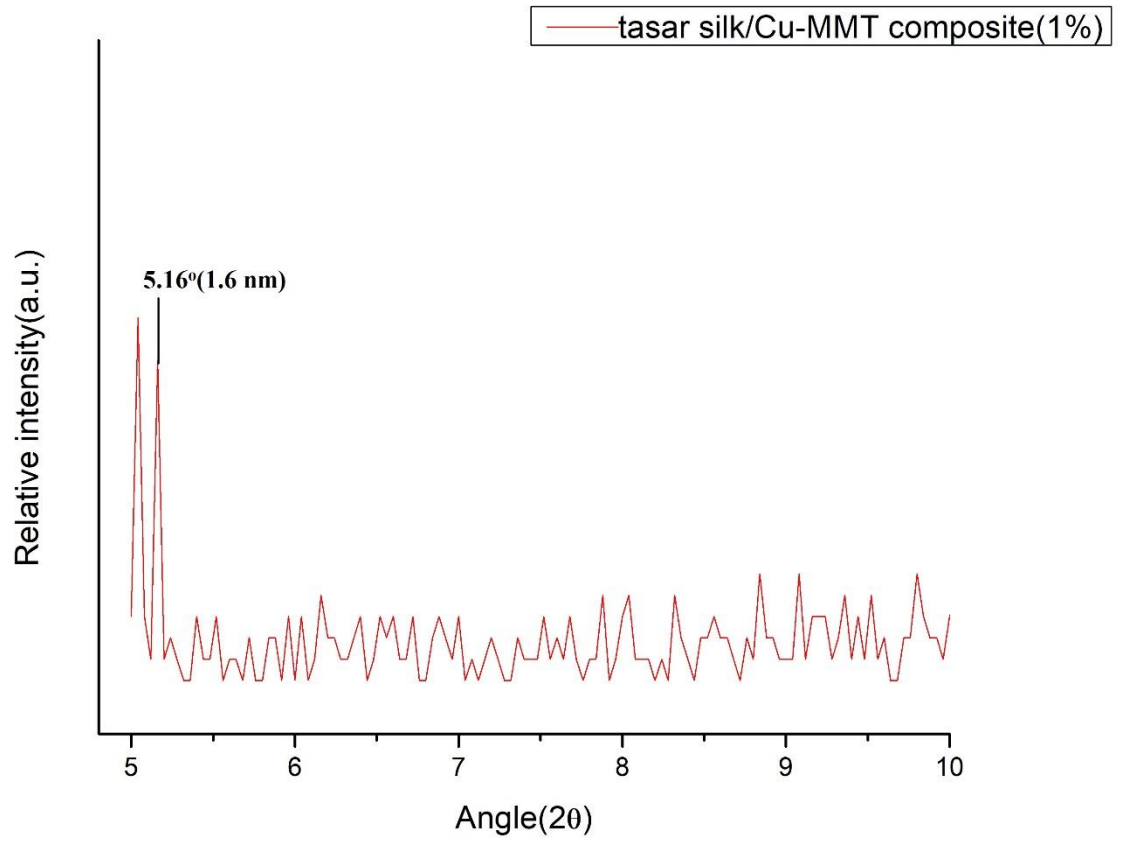


**Figure 15: XRD of tasar silk/ bioactive clay nanocomposite films**





## **CONCLUSION**

In this study, we developed a new organic/inorganic composite of regenerated tassar silk fibroin and MMT. Its microstructure and morphology has been characterized with the help of various characterization techniques including SEM-EDX, TEM, FTIR, and XRD measurement. The antibacterial properties has been evaluated against *E.coli* and *S.aureus* bacteria. XRD observations showed the intercalation of silk fibroin in between the silicate layers of MMT clay. FTIR showed the conformation of silk structure from silk I (random coil) to silk II ( $\beta$ -sheet). High-resolution TEM observations demonstrated the presence of the reduced silver nanoparticles on the surface of MMT silicate layers in the Ag-MMT clay. The clay has been found to be 1.25 nm thick and were interacted to the silk fibroins in unfamiliar way. Tassar silk fibroin/MMT composites showed good antibacterial properties with 1% weight percentage of modified clay in different tassar silk fibroin/MMT nanocomposite. SEM observations revealed that the nanocomposites possess three dimensional layered structure and EDX confirms the modification of clay by different cations exchanges (silver, copper and quaternary ammonium salt). This is the first report which reveals the studies of nanocomposite made from regenerated tassar silk fibroin with nanolayers of MMT. It is suggested that this nanocomposite can be a potential candidate for new biocompatible application as scaffold for tissue engineering like bone regeneration, because this composites possess antibacterial properties, biodegradable and biocompatible silk and osteo-inductive MMT. Furthermore the composite films would be advantageous in cell culture due to its especially high surface area and antibacterial properties.

## **REFERENCES:**

- [1] K. Malachová, P. Praus, Z. Rybková, and O. Kozák, “Antibacterial and antifungal activities of silver, copper and zinc montmorillonites,” *Appl. Clay Sci.*, vol. 53, no. 4, pp. 642–645, 2011.
- [2] S. K. Jou and N. A. N. N. Malek, “Characterization and antibacterial activity of chlorhexidine loaded silver-kaolinite,” *Appl. Clay Sci.*, vol. 127–128, pp. 1–9, 2016.
- [3] M. Hundáková, M. Valášková, V. Tomášek, E. Pazdziora, and K. Matějová, “Silver and/or copper vermiculites and their antibacterial effect,” *Acta Geodyn. Geomater.*, vol. 10, no. 1, pp. 97–104, 2013.
- [4] T. Posati *et al.*, “Innovative multifunctional silk fibroin and hydroxycalcite nanocomposites: A synergic effect of the components,” *Biomacromolecules*, vol. 15, no. 1, pp. 158–168, 2014.
- [5] Q. Dang, S. Lu, S. Yu, P. Sun, and Z. Yuan, “Silk fibroin/montmorillonite nanocomposites: Effect of pH on the conformational transition and clay dispersion,” *Biomacromolecules*, vol. 11, no. 7, pp. 1796–1801, 2010.
- [6] A. J. Mieszawska, J. G. Llamas, C. A. Vaiana, M. P. Kadakia, R. R. Naik, and D. L. Kaplan, “Clay enriched silk biomaterials for bone formation,” *Acta Biomater.*, vol. 7, no. 8, pp. 3036–3041, 2011.
- [7] L. Meinel *et al.*, “Silk based biomaterials to heal critical sized femur defects,” *Bone*, vol. 39, no. 4, pp. 922–931, 2006.
- [8] H. Zhao, X. Feng, S. Yu, W. Cui, and F. Zou, “Mechanical properties of silkworm cocoons,” vol. 46, pp. 9192–9201, 2005.
- [9] K. Sen and M. B. K, “Studies on Indian Silk . II . Structure – Property Correlations,” pp. 12–14, 2003.
- [10] K. Sen and M. B. K, “Studies on Indian Silk . I . Macrocharacterization and Analysis of Amino Acid Composition,” 2003.
- [11] R. Dash, S. Mukherjee, and S. C. Kundu, “Isolation, purification and characterization of silk protein sericin from cocoon peduncles of tropical tasar silkworm, *Antheraea mylitta*,”

- Int. J. Biol. Macromol.*, vol. 38, no. 3–5, pp. 255–258, 2006.
- [12] F. Sehnal and M. Žurovec, “Construction of silk fiber core in lepidoptera,” *Biomacromolecules*, vol. 5, no. 3, pp. 666–674, 2004.
- [13] A. Datta, A. K. Ghosh, and S. C. Kundu, “Purification and characterization of fibroin from the tropical Saturniid silkworm, *Antheraea mylitta*,” *Insect Biochem. Mol. Biol.*, vol. 31, no. 10, pp. 1013–1018, 2001.
- [14] R. Article, “Opportunities and Challenges in Exploring Indian Non-mulberry Silk for Biomedical Applications,” no. 1, pp. 85–101, 2017.
- [15] B. B. Mandal and S. C. Kundu, “Non-bioengineered silk fibroin protein 3D scaffolds for potential biotechnological and tissue engineering applications,” *Macromol. Biosci.*, vol. 8, no. 9, pp. 807–818, 2008.
- [16] B. Panilaitis, G. H. Altman, J. Chen, H. J. Jin, V. Karageorgiou, and D. L. Kaplan, “Macrophage responses to silk,” *Biomaterials*, vol. 24, no. 18, pp. 3079–3085, 2003.
- [17] E. Cukierman, R. Pankov, D. R. Stevens, and K. M. Yamada, “Taking cell-matrix adhesions to the third dimension,” *Science (80-. )*, vol. 294, no. 5547, pp. 1708–1712, 2001.
- [18] B. B. Mandal, T. Das, and S. C. Kundu, “Non-bioengineered silk gland fibroin micromolded matrices to study cell-surface interactions,” pp. 467–476, 2009.
- [19] B. B. Mandal and S. C. Kundu, “Biomaterials Calcium alginate beads embedded in silk fibroin as 3D dual drug releasing scaffolds,” *Biomaterials*, vol. 30, no. 28, pp. 5170–5177, 2009.
- [20] G. V. Joshi, B. D. Kevadiya, H. M. Mody, and H. C. Bajaj, “Confinement and controlled release of quinine on chitosan-montmorillonite bionanocomposites,” *J. Polym. Sci. Part A Polym. Chem.*, vol. 50, no. 3, pp. 423–430, 2012.
- [21] A. Sorrentino, G. Gorrasi, and V. Vittoria, “Potential perspectives of bio-nanocomposites for food packaging applications,” *Trends Food Sci. Technol.*, vol. 18, no. 2, pp. 84–95, 2007.
- [22] Q. H. Zeng, A. B. Yu, G. Q. (Max) Lu, and D. R. Paul, “Clay-Based Polymer

- Nanocomposites: Research and Commercial Development,” *J. Nanosci. Nanotechnol.*, vol. 5, no. 10, pp. 1574–1592, 2005.
- [23] W. Wang, S. Liao, M. Liu, Q. Zhao, and Y. Zhu, “Polymer Composites Reinforced by Nanotubes as Scaffolds for Tissue Engineering,” *Int. J. Polym. Sci.*, vol. 2014, pp. 1–14, 2014.
- [24] E. P. Giannes, “ADVANCED MATERIALS Polymer Layered Silicate Nanocomposites \*\*,” no. 1, pp. 29–35, 1996.
- [25] J. H. Choy, S. J. Choi, J. M. Oh, and T. Park, “Clay minerals and layered double hydroxides for novel biological applications,” *Appl. Clay Sci.*, vol. 36, no. 1–3, pp. 122–132, 2007.
- [26] W. F. Lee and Y. T. Fu, “Effect of montmorillonite on the swelling behavior and drug-release behavior of nanocomposite hydrogels,” *J. Appl. Polym. Sci.*, vol. 89, no. 13, pp. 3652–3660, 2003.
- [27] Á. Fudala, I. Pálinkó, and I. Kiricsi, “Preparation and Characterization of Hybrid Organic–Inorganic Composite Materials Using the Amphoteric Property of Amino Acids: Amino Acid Intercalated Layered Double Hydroxide and Montmorillonite,” *Inorg. Chem.*, vol. 38, no. 21, pp. 4653–4658, 2002.
- [28] T. Szabó *et al.*, “Adsorption of protamine and papain proteins on saponite,” *Clays Clay Miner.*, vol. 56, no. 5, pp. 494–504, 2008.
- [29] G. V. Joshi, H. A. Patel, B. D. Kevadiya, and H. C. Bajaj, “Montmorillonite intercalated with vitamin B1 as drug carrier,” *Appl. Clay Sci.*, vol. 45, no. 4, pp. 248–253, 2009.
- [30] T. Liu, X. F. Tian, Y. Zhao, and T. Gao, “Swelling of K<sup>+</sup>, Na<sup>+</sup> and Ca<sup>2+</sup>-montmorillonites and hydration of interlayer cations: A molecular dynamics simulation,” *Chinese Phys. B*, vol. 19, no. 10, pp. 1–7, 2010.
- [31] J. H. Park *et al.*, “Application of montmorillonite in bentonite as a pharmaceutical excipient in drug delivery systems,” *J. Pharm. Investig.*, vol. 46, no. 4, pp. 363–375, 2016.
- [32] J. Bujdák, “Effect of the layer charge of clay minerals on optical properties of organic dyes. A review,” *Appl. Clay Sci.*, vol. 34, no. 1–4, pp. 58–73, 2006.

- [33] P. Singla, R. Mehta, and S. N. Upadhyay, "Clay Modification by the Use of Organic Cations," vol. 2012, no. February, pp. 21–25, 2012.
- [34] C. M. Srivastava, "STUDIES ON REGENERATED NONMULBERRY SILK FILMS AND FIBERS," vol. 110042, no. 2, 2017.
- [35] Y. Kishimoto *et al.*, "Nanocomposite of silk fibroin nanofiber and montmorillonite: Fabrication and morphology," *Int. J. Biol. Macromol.*, vol. 57, pp. 124–128, 2013.